

Color-octet contributions for J/ψ inclusive production at B factories in soft gluon factorization

An-Ping Chen^a Xiao-Bo Jin^{b,c} Yan-Qing Ma^{b,d,e} Ce Meng^b

^a College of Physics and Communication Electronics, Jiangxi Normal University, Nanchang 330022, China

^b School of Physics and State Key Laboratory of Nuclear Physics and Technology, Peking University, Beijing 100871, China

^c Center of Advanced Quantum Studies, Department of Physics, Beijing Normal University, Beijing 100875, China

^d Center for High Energy physics, Peking University, Beijing 100871, China

^e Collaborative Innovation Center of Quantum Matter, Beijing 100871, China

E-mail: chenanping@jxnu.edu.cn, xiaobojin@pku.edu.cn, yqma@pku.edu.cn, mengce75@pku.edu.cn

ABSTRACT: We have studied color-octet contributions for J/ψ inclusive production at B factories, i.e., $e^+e^- \rightarrow J/\psi(^3P_J^{[8]}, ^1S_0^{[8]}) + X_{\text{non-}c\bar{c}}$, using the soft gluon factorization (SGF) approach, in which the J/ψ energy spectrum is expressed in a form of perturbatively calculable short-distance hard parts convoluted with one-dimensional soft gluon distributions (SGDs). The series of velocity corrections originated from kinematic effect can be naturally resummed in this approach. Short-distance hard parts have been calculated analytically to next-to-leading order in α_s . Renormalization group equations for SGDs have been derived and solved, which resums Sudakov logarithms originated from soft gluon emissions. Our final result gives a upper bound for color-octet matrix elements consistent with that extracted from hadron colliders. This may relieve the well-known universality problem in the NRQCD factorization.

As a comparison, we also analytically calculated short-distance hard parts in the NRQCD factorization, with Sudakov logarithms resummed by using soft collinear effective theory. The comparison shows that velocity corrections from kinematic effect, which have been resummed in SGF, are significant for phenomenological study. Furthermore, it is found that Sudakov logarithms originated from soft gluon emissions are very important, while it is not the case for Sudakov logarithms originated from jet function. Therefore, the partial Sudakov resummation in SGF has already captured the main physics.

Contents

1	Introduction	1
2	Soft gluon factorization formula	3
3	Perturbative calculation of the short-distance hard parts	7
3.1	The SGDs and the evolution equations	7
3.2	The perturbative differential cross sections	9
3.3	Matching the short-distance hard parts	12
4	NRQCD factorization	14
5	Phenomenology	21
6	Summary	24
7	Acknowledgments	25
A	Analytic expressions	25
B	x_{\min} dependence in SGF	29

1 Introduction

Although heavy quarkonium production has been widely studied in the nonrelativistic quantum chromodynamics (NRQCD) factorization [1], the underline mechanism is still under debate. The reason is that the NRQCD factorization can not provide a universal description of all quarkonium production data. In other words, long-distance matrix elements (LDMEs) in NRQCD are found to be not universal. It was argued in ref. [2] that the universality problem in NRQCD may be caused by the bad convergence of velocity expansion, which suffers from large high order relativistic corrections due to soft hadrons emission in the hadronization process. Resummation of these relativistic-correction terms will result in the so called soft gluon factorization (SGF) framework [2]. It was demonstrated in ref. [3] that the SGF is equivalent to the NRQCD factorization, but with a series of important relativistic corrections originated from kinematic effects resummed. As a result, the SGF approach should has a much better convergence in the velocity expansion, and thus may provide a reasonable description of heavy quarkonium production.

Besides exclusive processes [4], the SGF approach has been recently applied to calculate the fragmentation function of the gluon to a $^3S_1^{[8]}$ heavy quark-antiquark pair in ref. [5], which was expressed in a form of perturbative short-distance hard part convoluted with

one-dimensional ${}^3S_1^{[8]}$ soft gluon distribution (SGD). With a NLO calculation of the short-distance hard part, the authors demonstrated that the SGF is valid at NLO level. The renormalization group equation of the ${}^3S_1^{[8]}$ SGD was derived and solved, which resummed Sudakov logarithms to all orders in perturbation theory. A comparison with gluon fragmentation function calculated in NRQCD factorization indicates that the SGF formula resums a series of velocity corrections in NRQCD which are important for phenomenological study.

Color-octet (CO) contributions of the J/ψ production in e^+e^- annihilation, i.e., $e^+e^- \rightarrow J/\psi({}^3P_J^{[8]}, {}^1S_0^{[8]}) + X_{\text{non-}c\bar{c}}$, play an important role to understand the production mechanism of quarkonium. The J/ψ inclusive production at B factories have been measured by the BaBar and Belle collaborations [6–9] and have been studied in NRQCD factorization extensively [10–24]. In NRQCD factorization, the cross section $\sigma[e^+e^- \rightarrow J/\psi + X_{\text{non-}c\bar{c}}]$ at leading order (LO) in α_s includes color-singlet (CS) contribution $e^+e^- \rightarrow J/\psi({}^3S_1^{[1]}) + gg$, and CO contributions $e^+e^- \rightarrow J/\psi({}^3P_J^{[8]}, {}^1S_0^{[8]}) + g$. For J/ψ energy spectrum, the LO CO contribution predicts an apparent enhancement at the J/ψ maximum energy [11], but experiments did not show any enhancement at the endpoint region. It was then clear that large Sudakov logarithms appear at higher order invalidate the perturbative expansion of CO contributions. The behavior at the endpoint region can be qualitatively explained if the resummation of the Sudakov logarithms as well as nonperturbative effects are considered [25, 26]. On the other hand, the Belle measurement gives

$$\sigma[e^+e^- \rightarrow J/\psi + X_{\text{non-}c\bar{c}}] = (0.43 \pm 0.09 \pm 0.09) \text{ pb}, \quad (1.1)$$

which can be well saturated by CS channel with the next-to-leading order (NLO) in α_s correction [20, 21], $\mathcal{O}(v^2)$ relativistic correction [22, 23] and QED initial-state radiation effect [27], leaving little room for the contribution of CO channel. Even though, an upper bound of CO LDMEs can be obtained by setting the CS contribution to be zero, which at NLO level gives [24]

$$\langle \mathcal{O}^{J/\psi}({}^1S_0^{[8]}) \rangle + 4.0 \frac{\langle \mathcal{O}^{J/\psi}({}^3P_0^{[8]}) \rangle}{m_c^2} < (2.0 \pm 0.6) \times 10^{-2} \text{ GeV}^3. \quad (1.2)$$

However, this upper bound is much smaller than the value of CO LDMEs extracted from hadron colliders [28–32], which challenges the universality of LDMEs.

Because SGF has a better convergence in velocity expansion, in this paper we apply it to study the CO contributions of $e^+e^- \rightarrow J/\psi({}^3P_J^{[8]}, {}^1S_0^{[8]}) + X_{\text{non-}c\bar{c}}$. The rest of the paper is organized as follows. In section 2, we give a short review of SGF formula. Especially, we introduce a new lower cutoff x_{min} of momentum fraction and demonstrate that final result is insensitive to the value of x_{min} . In section 3, we present perturbative calculation in SGF. We also discuss the renormalization group equation (RGE) of SGDs. In section 4, we present perturbative calculation in NRQCD, and use the soft collinear effective theory (SCET) [26, 33–36] to resum large Sudakov logarithms to the NLL accuracy.

A comparison of phenomenological results obtained in SGF and NRQCD factorization are presented in section 5 and a summary is given in section 6. In appendix A we list some analytical expressions in perturbative calculation. Finally, we discuss the x_{min} dependence in appendix B.

2 Soft gluon factorization formula

We denote a four-vector a as

$$a^\mu = (a^0, a^1, a^2, a^3) = (a^0, \mathbf{a}).$$

We also use light-cone coordinates where a four-vector a can be expressed as

$$\begin{aligned} a^\mu &= (a^+, a^-, a^\perp) = (a^+, a^-, a_\perp), \\ a^+ &= (a^0 + a^3)/\sqrt{2}, \\ a^- &= (a^0 - a^3)/\sqrt{2}, \end{aligned}$$

where the subscript \perp denotes the perpendicular direction. Then scalar product of two four-vector a and b becomes

$$a \cdot b = a^+ b^- + a^- b^+ + a_\perp \cdot b_\perp.$$

We introduce a light-like vector $l^\mu = (0, 1, 0_\perp)$, so that $a \cdot l = a^+$.

Then in the rest frame of J/ψ we have

$$P_\psi^\mu = (M_\psi, \mathbf{0}), \quad q^\mu = (0, \mathbf{q}),$$

where P_ψ is the momentum of J/ψ , M_ψ is the mass of J/ψ and q is the half of the relative momentum of the heavy quark-antiquark pair in J/ψ , which is relate to the relative velocity v by $v = |\mathbf{q}|/m_c$, where m_c is the charm quark mass.

The SGF is equivalent to the NRQCD factorization but with a series of important relativistic corrections originated from kinematic effects resummed [3]. Beginning from the leading operator for a specific quantum number in NRQCD Lagrangian, e.g., $\psi^\dagger \chi$ (or $\psi^\dagger \sigma^i T^a \chi$, $\psi^\dagger \overleftrightarrow{\nabla}^i \chi$, and so on), one can construct powers suppressed operators like $\psi^\dagger \overleftrightarrow{\nabla}^2 \chi$, $\nabla^2(\psi^\dagger \chi)$ or $\psi^\dagger g \mathbf{E} \cdot \sigma \chi$ by inserting the relative derivative $\overleftrightarrow{\nabla}^2$, the total derivative ∇^2 , or the \mathbf{E} and \mathbf{B} fields. The first two kinds of insertions are originated from kinematic effects and they are chosen to be resummed. Using equations of motion, one can replace the relative derivatives $\overleftrightarrow{\nabla}^2$ and $\overleftrightarrow{\nabla}_0$ by total derivatives, which results in operators like $\nabla_0^{n_1} \nabla^{2n_2}(\psi^\dagger \chi)$. Then using integration by parts, one can eliminate all operators except that with $n_1 = n_2 = 0$. The price to pay is the introduction of the relative momentum between physical quarkonium and the intermediate heavy quark-antiquark pair into short-distance hard parts [3]. The final formula is the SGF proposed in ref. [2]. Note that, in the above derivation, one needs to introduce proper gluon fields to combine with spacetime derivatives to form gauge covariant derivatives.

In SGF, the production cross section of J/ψ in e^+e^- collisions can be expressed in following formula [2]:

$$(2\pi)^3 2P_\psi^0 \frac{d\sigma_\psi}{d^3P_\psi} = \sum_{n,n'} \int_{x_{\min}}^1 \frac{dx}{x^2} \hat{\sigma}_{[nn']}(P_\psi/x, s, m_c, x_{\min}/x, \mu_f) F_{[nn'] \rightarrow \psi}(x, M_\psi, m_c, \mu_f), \quad (2.1)$$

where x is the longitudinal momentum fraction defined as $x = P_\psi^+/P^+$ with P_ψ denoting the momentum of J/ψ and P denoting the total momentum of the intermediate $c\bar{c}$ pair. Different from the original form, we have introduced a lower cutoff x_{\min} for the x integration. This is allowed because, if x is too small, the intermediate $c\bar{c}$ pair will emit hard gluons during the hadronization process, which effect is perturbatively calculable. In appendix B we demonstrate that the production cross section is insensitive to the value of x_{\min} . In other words, the x_{\min} dependence of the integration limit cancels with the x_{\min} dependence of $\hat{\sigma}_{[nn']}$. This is not surprised at all because $\hat{\sigma}_{[nn']}$ is determined by matching the both sides of the above factorization formula. Therefore, as a special choice, one can also set $x_{\min} = 0$ [2].

In eq. (2.1), μ_f is the factorization scale, \sqrt{s} is the center-of-mass energy of the e^+e^- system, and the quarkonium state created by a_ψ^\dagger has standard relativistic normalization. $\hat{\sigma}_{[nn']}$ are perturbatively calculable short-distance hard parts that produce an intermediate $c\bar{c}$ pair with quantum numbers $n = 2S+1L_{J,J_z}^{[c]}$ and $n' = 2S'+1L'_{J',J'_z}^{[c']}$ in the amplitude and the complex-conjugate of the amplitude, respectively, with $c, c' = 1$ or 8 representing the color-singlet or color-octet state of the $c\bar{c}$ pair. $F_{[nn']\rightarrow\psi}$ are one-dimensional SGDs which are defined explicitly as [5]

$$F_{[nn']\rightarrow\psi}(x, M_\psi, m_c, \mu_f) = P_\psi^+ \int \frac{db^-}{2\pi} e^{-iP_\psi^+ b^-/x} \langle 0 | [\bar{\Psi} \mathcal{K}_n \Psi]^\dagger(0) [a_\psi^\dagger a_\psi] [\bar{\Psi} \mathcal{K}_{n'} \Psi](b^-) | 0 \rangle_S, \quad (2.2)$$

where Ψ denotes the Dirac field of heavy quark. The subscript ‘‘S’’ means that the field operators in the definition are the operators obtained in small momentum region. In addition, we define ‘‘S’’ to select only leading power terms in threshold expansion[5], that is the expansion in the limit $(P - P_\psi)^+ = (1 - x)P^+ \rightarrow 0$.

In general the state n can be different from the state n' , but for the case of producing a polarization summed J/ψ , there are constraints $c = c', S = S', J = J', J_z = J'_z$ and $|L - L'| = 0, 2, 4, \dots$ [2, 37]. While in this work, we only consider the case $n = n'$ with $n = 1S_0^{[8]}$ or $3P_{J,\lambda}^{[8]}$, where are the most important color-octet contributions for J/ψ production at e^+e^- collision. The corresponding projection operators \mathcal{K}_n , which define the intermediate state n , are given by [2]

$$\mathcal{K}_{1S_0^{[8]}}(rb^-) = \frac{\sqrt{M_\psi}}{M_\psi + 2m_c} \frac{M_\psi + \not{P}_\psi}{2M_\psi} \mathcal{C}_a^{[8]\gamma_5} \frac{M_\psi - \not{P}_\psi}{2M_\psi}, \quad (2.3a)$$

$$\mathcal{K}_{3P_{J,\lambda}^{[8]}}(rb^-) = \frac{\sqrt{M_\psi}}{M_\psi + 2m_c} \frac{M_\psi + \not{P}_\psi}{2M_\psi} \mathcal{C}_a^{[8]} \mathcal{E}_{J,\lambda}^{\mu\nu} \gamma_\mu \left(-\frac{i}{2} \right) \overleftrightarrow{D}_\nu \frac{M_\psi - \not{P}_\psi}{2M_\psi}, \quad (2.3b)$$

where D_μ is the gauge covariant derivative with $\bar{\Psi} \overleftrightarrow{D}_\mu \Psi = \bar{\Psi} (D_\mu \Psi) - (D_\mu \bar{\Psi}) \Psi$. The color operator is given by

$$\mathcal{C}_a^{[8]} = \sqrt{2} T^{\bar{a}} \Phi_l(rb^-)_{\bar{a}a}, \quad (2.4)$$

with gauge link $\Phi_l(rb^-)_{\bar{a}a}$ defined along the l^μ direction,

$$\Phi_l(rb^-) = \mathcal{P} \exp \left[-ig_s \int_0^\infty d\xi l \cdot A(rb^- + \xi l) \right], \quad (2.5)$$

where \mathcal{P} denotes path ordering and $A^\mu(x)$ is gluon field in the adjoint representation: $[A^\mu(x)]_{ac} = if^{abc}A_b^\mu(x)$. $\mathcal{E}_{J,\lambda}$ are polarization tensors for ${}^3P_{J,\lambda}^{[8]}$ states, with the following summation rules,

$$\sum_{\lambda} \mathcal{E}_{0,\lambda}^{\mu\nu} \mathcal{E}_{0,\lambda}^{*\mu'\nu'} = \frac{1}{d-1} \mathbb{P}^{\mu\nu} \mathbb{P}^{\mu'\nu'}, \quad (2.6a)$$

$$\sum_{\lambda} \mathcal{E}_{1,\lambda}^{\mu\nu} \mathcal{E}_{1,\lambda}^{*\mu'\nu'} = \frac{1}{2} [\mathbb{P}^{\mu\mu'} \mathbb{P}^{\nu\nu'} - \mathbb{P}^{\mu\nu'} \mathbb{P}^{\mu'\nu}], \quad (2.6b)$$

$$\sum_{\lambda} \mathcal{E}_{2,\lambda}^{\mu\nu} \mathcal{E}_{2,\lambda}^{*\mu'\nu'} = \frac{1}{2} [\mathbb{P}^{\mu\mu'} \mathbb{P}^{\nu\nu'} + \mathbb{P}^{\mu\nu'} \mathbb{P}^{\mu'\nu}] - \frac{1}{d-1} \mathbb{P}^{\mu\nu} \mathbb{P}^{\mu'\nu'}, \quad (2.6c)$$

$$\sum_{J,\lambda} \mathcal{E}_{J,\lambda}^{\mu\nu} \mathcal{E}_{J,\lambda}^{*\mu'\nu'} = \mathbb{P}^{\mu\mu'} \mathbb{P}^{\nu\nu'}, \quad (2.6d)$$

where d is the space-time dimension, the spin projection operator $\mathbb{P}^{\mu\nu}$ is defined as

$$\mathbb{P}^{\mu\nu} = -g^{\mu\nu} + \frac{P_\psi^\mu P_\psi^\nu}{M_\psi^2}. \quad (2.7)$$

For energy distribution, we can rewrite eq. (2.1) as

$$\begin{aligned} \frac{d\sigma_{J/\psi}}{dz} &= \sum_n \int_{\max[(z+\sqrt{z^2-4r})/2, x_{\min}] }^1 \frac{dx}{x} H_{[n]}(\hat{z}, M_\psi/x, s, m_c, x_{\min}/x, \mu_f) \\ &\times F_{[n] \rightarrow \psi}(x, M_\psi, m_c, \mu_f), \end{aligned} \quad (2.8)$$

where we denote $[n] \equiv [nn]$, with $n = 1S_0^{[8]}$ or ${}^3P_{J,\lambda}^{[8]}$, and new variables are defined as

$$z \equiv \frac{2E_\psi}{\sqrt{s}}, \quad \hat{z} \equiv \frac{z}{x} = \frac{2E_\psi}{x\sqrt{s}}, \quad r \equiv \frac{M_\psi^2}{s}. \quad (2.9)$$

The variables E_ψ/x and M_ψ/x in the hard part correspond to energy $E_{c\bar{c}}$ and invariant mass $M_{c\bar{c}}$ of the intermediate $c\bar{c}$ pair, respectively.

In above factorization formula, the short-distance hard parts $H_{[n]}$ are determined by the matching procedure [2, 5]. To this end, we replace the final-state J/ψ by an on-shell $c\bar{c}$ pair with certain quantum number n and momenta

$$p_c = \frac{1}{2}P_\psi + q, \quad p_{\bar{c}} = \frac{1}{2}P_\psi - q. \quad (2.10)$$

On-shell conditions $p_c^2 = p_{\bar{c}}^2 = m_c^2$ result in

$$P_\psi \cdot q = 0, \quad q^2 = m_c^2 - P_\psi^2/4. \quad (2.11)$$

To project the final-state $c\bar{c}$ pair to the state n , we replace spinors of the $c\bar{c}$ by following projector

$$\Pi[n] = \frac{2}{\sqrt{M_\psi(M_\psi + 2m_c)}} (\not{p}_{\bar{c}} - m_c) \frac{M_\psi - \not{P}_\psi}{2M_\psi} \tilde{\Gamma}_n^s \tilde{\mathcal{C}}^{[c]} \frac{M_\psi + \not{P}_\psi}{2M_\psi} (\not{p}_c + m_c), \quad (2.12)$$

where, for $n = 1S_0^{[8]}$ or $3P_{J,\lambda}^{[8]}$, the color operator and spin operator are given by

$$\tilde{\mathcal{C}}^{[8]} = \sqrt{\frac{2}{N_c^2 - 1}} T^a, \quad (2.13a)$$

$$\tilde{\Gamma}_{1S_0^{[8]}}^s = \gamma_5, \quad (2.13b)$$

$$\tilde{\Gamma}_{3P_{J,\lambda}^{[8]}}^s = (d-1) \frac{q_\alpha}{|\mathbf{q}|^2} \mathcal{E}_{J,\lambda}^{*\alpha\mu} \gamma_\mu. \quad (2.13c)$$

The factor $\sqrt{N_c^2 - 1}$ is to average over color-octet states. We insert the perturbative expansions

$$\frac{d\sigma_{c\bar{c}[n]}}{dz} = \frac{d\sigma_{c\bar{c}[n]}^{LO}}{dz} + \frac{d\sigma_{c\bar{c}[n]}^{NLO}}{dz} + \dots, \quad (2.14a)$$

$$F_{[n'] \rightarrow c\bar{c}[n]} = F_{[n'] \rightarrow c\bar{c}[n]}^{LO} + F_{[n'] \rightarrow c\bar{c}[n]}^{NLO} + \dots, \quad (2.14b)$$

$$H_{[n']} = H_{[n']}^{LO} + H_{[n']}^{NLO} + \dots \quad (2.14c)$$

into the factorization formula eq. (2.8). At leading order we have[2]

$$F_{[n'] \rightarrow c\bar{c}[n]}^{LO}(x, M_\psi, m_c, \mu_f) = \delta_{n'n} \delta(1-x), \quad (2.15)$$

which results in following matching relations up to NLO

$$H_{[n]}^{LO}(z, M_\psi, s, m_c, x_{\min}, \mu_f) = \frac{d\sigma_{c\bar{c}[n]}^{LO}}{dz}(z, M_\psi, s, m_c), \quad (2.16a)$$

$$H_{[n]}^{NLO}(z, M_\psi, s, m_c, x_{\min}, \mu_f) = \frac{d\sigma_{c\bar{c}[n]}^{NLO}}{dz}(z, M_\psi, s, m_c) - \sum_{n'} \int_{\max[\frac{\sqrt{z^2-4r+z}}{2}, x_{\min}]}^1 \frac{dx}{x} \frac{d\sigma_{c\bar{c}[n']}}{dz} \left(\frac{z}{x}, \frac{M_\psi}{x}, s, m_c \right) F_{[n'] \rightarrow c\bar{c}[n]}^{NLO}(x, M_\psi, m_c, \mu_f). \quad (2.16b)$$

In the SGF, velocity expansion is achieved by expanding m_c^2 in the hard parts $H_{[n]}$ around $M_\psi^2/4x^2$, which results in

$$\begin{aligned} \frac{d\sigma_{J/\psi}}{dz} &= \sum_{i=0} \sum_n \int_{\max[(z+\sqrt{z^2-4r})/2, x_{\min}]}^1 \frac{dx}{x} H_{[n]}^{(i)}(\hat{z}, M_\psi/x, s, x_{\min}/x, \mu_f) \left(m_c^2 - \frac{M_\psi^2}{4x^2} \right)^i \\ &\times F_{[n] \rightarrow \psi}(x, M_\psi, m_c, \mu_f). \end{aligned} \quad (2.17)$$

In ref. [5], an explicit NLO calculation shows that the above kind of velocity expansion has good convergence, and the lowest order in the expansion can give a very good approximation of the full result. Therefore, to simplify the perturbative calculation, we only consider the contribution of $H_{[n]}^{(0)}$ here, with

$$H_{[n]}^{(0)}(z/x, M_\psi/x, s, x_{\min}/x, \mu_f) = H_{[n]}(z/x, M_\psi/x, s, m_c, x_{\min}/x, \mu_f)|_{m_c=M_\psi/2x}. \quad (2.18)$$

Based on eqs. (2.18) and (2.16), we can calculate the short-distance hard parts perturbatively. Especially, we can set $m_c = M_\psi/2x$ in the integrand level before performing loop integration.

3 Perturbative calculation of the short-distance hard parts

3.1 The SGDs and the evolution equations

To obtain short-distance hard parts $H_{[n]}^{(0)}$ up to NLO, we need first to calculate the perturbative SGDs. One-loop correction for the perturbative SGDs can be derived by following the calculation details of color-octet 3S_1 SGD given in [5]. As we keep only the leading order in the velocity expansion, we can expand m_c^2 around $M_\psi^2/4$ before performing the loop integration and phase space integration. The calculation is straightforward and we get

$$\begin{aligned}
F_{[1S_0^{[8]}] \rightarrow c\bar{c}[1S_0^{[8]}]}(x, M_\psi, m_c, \mu_f) = & \delta(1-x) + \frac{\alpha_s N_c}{4\pi} \left[\frac{4x}{(1-x)_+} \ln\left(\frac{x^2 \mu_f^2 e^{-1}}{M_\psi^2}\right) \right. \\
& - 8x \left(\frac{\ln(1-x)}{1-x} \right)_+ - \delta(1-x) \left(\ln^2\left(\frac{\mu_f^2 e^{-1}}{M_\psi^2}\right) + \frac{\pi^2}{6} - 1 \right) \\
& \left. - \frac{1}{N_c^2} \frac{\pi^2}{\Delta} \delta(1-x) \right] + \mathcal{O}(\Delta), \tag{3.1a}
\end{aligned}$$

$$\begin{aligned}
F_{[{}^3P_{J',\lambda'}^{[8]}] \rightarrow c\bar{c}[{}^3P_{J,\lambda}^{[8]}]}(x, M_\psi, m_c, \mu_f) = & \delta_{J',J} \delta_{\lambda',\lambda} \left\{ \delta(1-x) + \frac{\alpha_s N_c}{4\pi} \left[\frac{4x}{(1-x)_+} \ln\left(\frac{x^2 \mu_f^2 e^{-1}}{M_\psi^2}\right) \right. \right. \\
& - 8x \left(\frac{\ln(1-x)}{1-x} \right)_+ - \delta(1-x) \left(\ln^2\left(\frac{\mu_f^2 e^{-1}}{M_\psi^2}\right) + \frac{\pi^2}{6} - 1 \right) \\
& \left. \left. - \frac{1}{N_c^2} \frac{\pi^2}{\Delta} \delta(1-x) \right] \right\} + \mathcal{O}(\Delta). \tag{3.1b}
\end{aligned}$$

Here $\Delta = \sqrt{1 - 4m_c^2/M_\psi^2}$, the ‘‘plus’’ functions are defined in the standard way through

$$\int_z^1 dx f(x) \left[\frac{\ln^m(1-x)}{1-x} \right]_+ = \int_z^1 dx [f(x) - f(1)] \frac{\ln^m(1-x)}{1-x} + \frac{f(1)}{m+1} \ln^{m+1}(1-z), \tag{3.2}$$

where $f(x)$ is a well-behaved regular function.

In SGF, the general form of RGEs for SGDs is given by [5]

$$\begin{aligned}
\frac{d}{d \ln \mu_f} F_{[n] \rightarrow \psi}(x, M_\psi, m_c, \mu_f) = & \sum_{n'} \int_x^1 \frac{dy}{y} \mathbf{K}_{[n]}^{[n']}(x/y, M_\psi/y, m_c, \mu_f) \\
& \times F_{[n'] \rightarrow \psi}(y, M_\psi, m_c, \mu_f), \tag{3.3}
\end{aligned}$$

where the evolution kernel can also be expressed in the velocity expansion series

$$\mathbf{K}_{[n]}^{[n']}(x/y, M_\psi/y, m_c, \mu_f) = \sum_{i=0} \mathbf{K}_{[n]}^{[n'],(i)}(x/y, M_\psi/y, \mu_f) \left(m_c^2 - \frac{M_\psi^2}{4y^2} \right)^i. \tag{3.4}$$

Using above perturbative SGD results we can obtain evolution kernel $\mathbf{K}_{[n]}^{[n'],(0)}$ at LO in α_s by matching both sides of the RGE,

$$\mathbf{K}_{[1S_0^{[8]}]}^{[1S_0^{[8]}],(0),LO}(x, M_\psi, \mu_f) = \frac{\alpha_s}{4\pi} \left[2\Gamma_0^F \left(\frac{x}{(1-x)_+} - \ln \frac{\mu_f}{M_\psi} \delta(1-x) \right) + \gamma_0^F \delta(1-x) \right], \tag{3.5a}$$

$$\mathbf{K}_{[3P_{J,\lambda}^{[8]}]}^{[3P_{J',\lambda'}^{[8]}],(0),LO}(x, M_\psi, \mu_f) = \frac{\alpha_s}{4\pi} \left[2\Gamma_0^F \left(\frac{x}{(1-x)_+} - \ln \frac{\mu_f}{M_\psi} \delta(1-x) \right) + \gamma_0^F \delta(1-x) \right] \times \delta_{JJ'} \delta_{\lambda\lambda'}, \quad (3.5b)$$

where

$$\Gamma_0^F = 4N_c, \quad \gamma_0^F = 4N_c. \quad (3.6)$$

For the convenience of discussion, here we give some details of solving the above RGEs. We take $1S_0^{[8]}$ SGD as an example. Following the discussion in ref. [5], we rewrite the RGE as a function of the variable $\omega_0 = (1-x)/x$, which is

$$\begin{aligned} & \frac{d}{d \ln \mu_f} F_{[1S_0^{[8]}] \rightarrow \psi}(\omega_0, M_\psi, m_c, \mu_f) \\ &= \int_0^{\omega_0} d\omega'_0 \frac{\alpha_s}{4\pi} \left[2\Gamma_0^F \left(\left[\frac{1}{\omega_0 - \omega'_0} \right]_+ - \ln \frac{\mu_f}{M_\psi} \delta(\omega_0 - \omega'_0) \right) + \gamma_0^F \delta(\omega_0 - \omega'_0) \right] \\ & \times F_{[1S_0^{[8]}] \rightarrow \psi}(\omega'_0, M_\psi, m_c, \mu_f), \end{aligned} \quad (3.7)$$

where $\omega'_0 = (1-y)/y$. ω_0 (or ω'_0) is actually the longitudinal momentum fraction of the emitted soft gluons, and it takes values between 0 and ∞ . To solve the above equation, it is convenient to perform the Laplace transformation, which, together with its inverse, is given by

$$\tilde{f}(\nu) = \int_0^\infty d\omega_0 e^{-\omega_0 \nu} f(\omega_0), \quad \text{and} \quad f(\omega_0) = \frac{1}{2\pi i} \int_{c-i\infty}^{c+i\infty} d\nu e^{\omega_0 \nu} \tilde{f}(\nu), \quad (3.8)$$

where the constant c is chosen to be larger than the real part of the rightmost singularity of $\tilde{f}(s)$. Performing a Laplace transform in eq. (3.7) we obtain a RGE in Laplace space

$$\begin{aligned} \frac{d}{d \ln \mu_f} \tilde{F}_{[1S_0^{[8]}] \rightarrow \psi}(\nu, M_\psi, m_c, \mu_f) &= \frac{\alpha_s}{4\pi} \left(-2\Gamma_0^F \ln \frac{\bar{\nu} \mu_f}{M_\psi} + \gamma_0^F \right) \\ & \times \tilde{F}_{[1S_0^{[8]}] \rightarrow \psi}(\nu, M_\psi, m_c, \mu_f), \end{aligned} \quad (3.9)$$

where $\bar{\nu} = \nu e^{\gamma_E}$, γ_E is the Euler's constant. Solving the above equation, we then obtain [5]

$$\begin{aligned} \tilde{F}_{[1S_0^{[8]}] \rightarrow \psi}(\nu, M_\psi, m_c, \mu_r) &= \left[1 + \frac{\alpha_s(\mu_r) N_c}{4\pi} \left(-4 \ln^2 \frac{\mu_r e^{\gamma_E}}{M_\psi} + 4 \ln \frac{\mu_r e^{\gamma_E}}{M_\psi} - \frac{5\pi^2}{6} \right) \right] \\ & \times \exp \left[h_0(\mu_r, \chi_0) \right] \tilde{F}^{\text{mod}}[1S_0^{[8]}](\nu). \end{aligned} \quad (3.10)$$

Here we evolved the SGD from the initial scale μ_r/ν to the scale μ_r . $\tilde{F}^{\text{mod}}[1S_0^{[8]}](\nu)$ is a model introduced to describe the nonperturbative effects at the initial scale μ_r/ν . And the evolution function h_0 is given by

$$h_0(\mu_r, \chi_0) = \frac{2\pi\Gamma_0^F}{\beta_0^2} \frac{1}{\alpha_s(\mu_r)} \left(-(1-2\chi_0) \ln(1-2\chi_0) - 2\chi_0 \right) - \frac{\gamma_0^F}{2\beta_0} \ln(1-2\chi_0)$$

$$+ \frac{\Gamma_0^F}{\beta_0} \ln(1 - 2\chi_0) \ln \frac{\mu_r e^{\gamma_E}}{M_S}, \quad (3.11)$$

with

$$\chi_0 = \frac{\alpha_s(\mu_r)\beta_0}{4\pi} \ln \nu, \quad (3.12)$$

where $\beta_0 = (11/3)C_A - (4/3)T_F n_f$, n_f is the number of active quark flavors and we choose $n_f = 3$. For the SU(3) color factors we have $T_F = 1/2$, $C_F = 4/3$ and $C_A = 3$. The presence of $\ln(1 - 2\chi_0)$ in eq. (3.11) leads to the Landau singularity at the branch point

$$\nu_1^L = \exp\left(\frac{2\pi}{\beta_0\alpha_s(\mu_r)}\right). \quad (3.13)$$

The Landau singularity can be avoided by performing following replacement in eqs. (3.11) and (3.12) as discussed in refs. [38, 39]

$$\chi_0 \rightarrow \chi_{0*} = \frac{\alpha_s(\mu_r)\beta_0}{4\pi} \ln\left(\frac{\nu}{1 + \nu/\nu_{1*}^L}\right), \quad \nu_{1*}^L = \nu_1^L/a, \quad (3.14)$$

where a is a parameter of order 1 but not smaller than 1. Such a replacement prevents χ_0 from entering the nonperturbative regime. And the nonperturbative effects would be compensated by the model $\tilde{F}^{\text{mod}}[{}^1S_0^{[8]}](\nu)$. Finally, with the help of the numerical inverse Laplace transformation, we can transform eq. (3.10) back to momentum space,

$$F_{[{}^1S_0^{[8]}] \rightarrow \psi}(x, M_\psi, m_c, \mu_r) = \frac{1}{2\pi i} \int_{c-i\infty}^{c+i\infty} d\nu e^{(1/x-1)\nu} \tilde{F}_{[{}^1S_0^{[8]}] \rightarrow \psi}(\nu, M_\psi, m_c, \mu_r). \quad (3.15)$$

The evolution of ${}^3P_{J,\lambda}^{[8]}$ SGD can be solved similarly.

3.2 The perturbative differential cross sections

We will calculate the perturbative differential cross sections of e^+e^- annihilate to the $c\bar{c}$ pair in state ${}^1S_0^{[8]}$ and ${}^3P^{[8]}$. For P-wave channel, we only calculate the polarization-summed hard part defined by

$$H_{[{}^3P^{[8]}]}^{(0)}(\hat{z}, M_\psi/x, s, x_{\min}/x, \mu_f) = \frac{1}{(d-1)^2} \sum_{J,\lambda} H_{[{}^3P_{J,\lambda}^{[8]}]}^{(0)}(\hat{z}, M_\psi/x, s, x_{\min}/x, \mu_f). \quad (3.16)$$

We choose the e^+e^- center-of-mass frame to perform the calculation.

At LO, the Feynman diagrams are given in figure 1. Replacing the spinors of $c\bar{c}$ in the amplitude with the projectors in eq. (2.12) and integrating over the solid angle of q in the $c\bar{c}$ rest frame, we can derive

$$\frac{d\sigma_S^{LO}}{dz}(z, M_\psi, s, m_c) = \frac{256\pi^2\alpha^2\alpha_s e_c^2 m_c^2 \mathcal{T}^2}{3s^2 M_\psi^3} \frac{1-r}{1+r} \delta(1-\bar{z}), \quad (3.17)$$

for the ${}^1S_0^{[8]}$ channel. Here

$$\bar{z} = \frac{z}{1+r}, \quad \mathcal{T} = {}_2F_1\left(\frac{1}{2}, 1, \frac{3}{2} - \epsilon, \Delta^2\right). \quad (3.18)$$

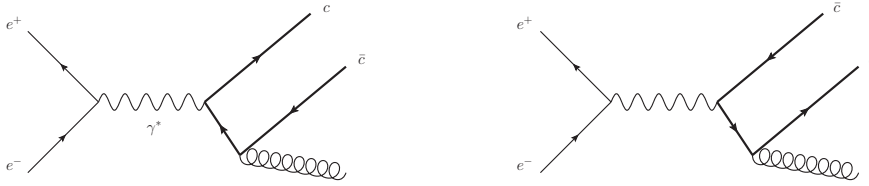


Figure 1. LO Feynman diagrams for $e^+e^- \rightarrow c\bar{c}(^1S_0^{[8]}, c\bar{c}[^3P^{[8]}]) + g$.

For convenience, we use S and P to represent the $c\bar{c}[^1S_0^{[8]}]$ and $c\bar{c}[^3P^{[8]}]$ states, respectively. For the P-wave contribution, we list the result in appendix [A](#).

We take the S-wave contribution as an example to describe the calculation at NLO. Some typical NLO Feynman diagrams are showed in figure [2](#). The differential cross section

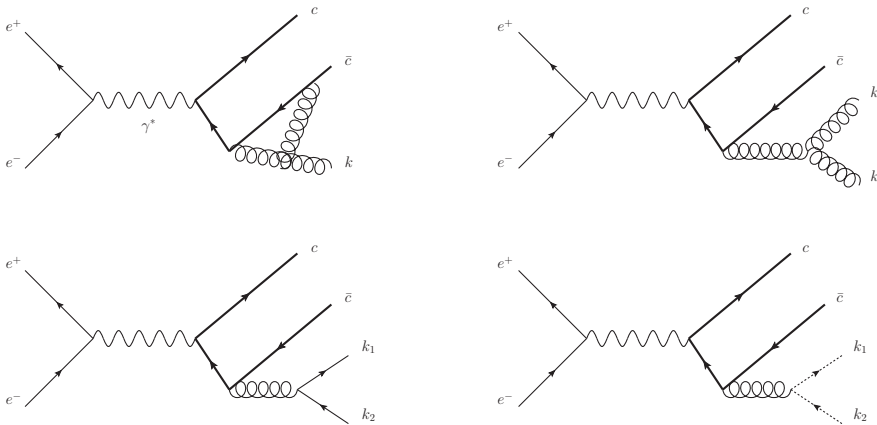


Figure 2. Representative NLO Feynman diagrams for the $c\bar{c}[^1S_0^{[8]}]$ production from e^+e^- annihilation.

is given by

$$\frac{d\sigma_S^{NLO}}{dz} = \frac{d\sigma_{\text{virtual}}}{dz} + \frac{d\sigma_{\text{real}}}{dz}, \quad (3.19)$$

with

$$\frac{d\sigma_{\text{virtual}}}{dz} = \frac{(d-2)e^2}{4(d-1)s^2} \int d\Phi_2 \sum 2\text{Re}(\mathcal{M}_{\text{Born}}^* \mathcal{M}_{\text{virtual}}) \quad (3.20a)$$

$$\frac{d\sigma_{\text{real}}}{dz} = \frac{(d-2)e^2}{4(d-1)s^2} \int d\Phi_3 \sum |\mathcal{M}_{\text{real}}|^2, \quad (3.20b)$$

where we have use Lorentz covariance and gauge invariance to relate the cross section in e^+e^- annihilation to the decay rate of a virtual photon. Therefore, $\mathcal{M}_{\text{Born}}$ denotes the tree-level amplitude for $\gamma^* \rightarrow c\bar{c}(^1S_0^{[8]}) + g$, $\mathcal{M}_{\text{virtual}}$ denotes the one-loop amplitude for $\gamma^* \rightarrow c\bar{c}(^1S_0^{[8]}) + g$ and $\mathcal{M}_{\text{real}}$ is the amplitude for real correction of $\gamma^* \rightarrow c\bar{c}(^1S_0^{[8]}) + X$, where X can be two gluons, a light quark-antiquark pair or a ghost-ghost pair. \sum means summation over the polarizations final states and initial state virtual photon. $d\Phi_{2(3)}$ means

two-body (three-body) phase space which are given by

$$d\Phi_2 = \frac{d^{d-1}\mathbf{P}_\psi}{(2\pi)^{d-1}2E_\psi} \frac{d^{d-1}\mathbf{k}}{(2\pi)^{d-1}2k^0} (2\pi)^d \delta^d(q_\gamma - P_\psi - k) \delta(z - \frac{2E_\psi}{\sqrt{s}}), \quad (3.21)$$

$$d\Phi_3 = \frac{1}{N_s} \frac{d^{d-1}\mathbf{P}_\psi}{(2\pi)^{d-1}2E_\psi} \frac{d^{d-1}\mathbf{k}_1}{(2\pi)^{d-1}2k_1^0} \frac{d^{d-1}\mathbf{k}_2}{(2\pi)^{d-1}2k_2^0} (2\pi)^d \delta^d(q_\gamma - P_\psi - k_1 - k_2) \delta(z - \frac{2E_\psi}{\sqrt{s}}), \quad (3.22)$$

where q_γ is the momentum of γ^* , k and k_i ($i = 1, 2$) represent the momentum of emitted gluon, light quark or ghost, as showed in figure 2, and N_s is the symmetry factor for final-state particles.

In the calculation, we use FeynArts [40] to generate Feynman diagrams and amplitudes, and then use in-house code to contract Lorentz indices and carry out traces of Dirac matrices. According to eqs. (2.16), (2.18), we expand m_c^2 in the amplitudes around $M_\psi^2/4$ and neglect the terms of $\mathcal{O}(|\mathbf{q}|)$ before performing loop integration and phase space integration. We use the reverse unitary technique [41–43] to transform the delta functions to propagator denominators,

$$\delta(x) = \frac{1}{2\pi} \lim_{\varepsilon \rightarrow 0} \left(\frac{1}{x + i\varepsilon} - \frac{1}{x - i\varepsilon} \right), \quad (3.23)$$

then phase space integration can be treated similar as loop integration. We use the integration-by-parts (IBP) method [44, 45] and employ the package FIRE5 [46] to perform the reduction of loop integrals, which express cross sections as linear combinations of master integrals (MIs). To calculate these MIs, we can set up differential equations with respect to r [47, 48],

$$\frac{\partial}{\partial r} \mathbf{I}(r, \epsilon) = \mathbf{A}(r, \epsilon) \mathbf{I}(r, \epsilon). \quad (3.24)$$

The boundary conditions at $r = 1$ can be calculated by using the method of region [49]. We then use the algorithm in [50] to transform eq. (3.24) to the ϵ -form [51]. By solving the system, we obtain the MIs which are expressed by Goncharov polylogarithms [52]. We further simplify the expressions by using the package PolyLogTools[53]. Combining the IBP coefficients and the MIs we obtain expressions of the virtual and real corrections.

The UV divergence in virtual correction can be removed by the renormalization. We choose the renormalization constants Z_2 , Z_m , Z_3 that correspond the charm quark field, the charm quark mass and the gluon field respectively in the on-mass-shell (OS) scheme, and choose Z_g that corresponds the QCD coupling in the minimal-subtractions ($\overline{\text{MS}}$) scheme,

$$\begin{aligned} \delta Z_2^{\text{OS}} &= -C_F \frac{\alpha_s}{4\pi} \left[\frac{1}{\epsilon_{\text{UV}}} + \frac{2}{\epsilon_{\text{IR}}} - 3\gamma_E + 3 \ln \frac{4\pi\mu^2}{m_c^2} + 4 \right] + \mathcal{O}(\alpha_s^2), \\ \delta Z_m^{\text{OS}} &= -3C_F \frac{\alpha_s}{4\pi} \left[\frac{1}{\epsilon_{\text{UV}}} - \gamma_E + \ln \frac{4\pi\mu^2}{m_c^2} + \frac{4}{3} \right] + \mathcal{O}(\alpha_s^2), \\ \delta Z_3^{\text{OS}} &= \frac{\alpha_s}{4\pi} (\beta_0 - 2C_A) \left[\frac{1}{\epsilon_{\text{UV}}} - \frac{1}{\epsilon_{\text{IR}}} \right] + \mathcal{O}(\alpha_s^2), \\ \delta Z_g^{\overline{\text{MS}}} &= -\frac{\beta_0}{2} \frac{\alpha_s}{4\pi} \left[\frac{1}{\epsilon_{\text{UV}}} - \gamma_E + \ln(4\pi) \right] + \mathcal{O}(\alpha_s^2). \end{aligned} \quad (3.25)$$

Combining the virtual and real corrections, we get the differential cross section. The P-wave contribution can be calculated similarly. Expressions of S-wave and P-wave contributions are given by

$$\begin{aligned} \frac{d\sigma_S^{NLO}}{dz} = & \sigma_S^0 \left\{ \left(\frac{\alpha_s}{4\pi} R_S(M_\psi, r, \mu_r) - \frac{\alpha_s}{4\pi} \frac{1}{C_A} \frac{\pi^2}{\Delta} \right) \delta(1-\bar{z}) \right. \\ & + \frac{\alpha_s}{4\pi} \left[\left(4C_A \ln \frac{\left(\sqrt{(r+1)^2 \bar{z}^2 - 4r} + r\bar{z} - 2r + \bar{z} \right)^2}{4r(r+1)} - P[r, \bar{z}] (4C_A + \beta_0) \right) \right. \\ & \left. \left. \times \left[\frac{1}{1-\bar{z}} \right]_+ - 4C_A \left[\frac{\ln(1-\bar{z})}{1-\bar{z}} \right]_+ + P[r, \bar{z}] \mathcal{R}_S(\bar{z}, M_\psi, r, \mu_r) \right] \right\} + \mathcal{O}(\Delta), \end{aligned} \quad (3.26a)$$

$$\begin{aligned} \frac{d\sigma_P^{NLO}}{dz} = & \sigma_P^0 \left\{ \left(\frac{\alpha_s}{4\pi} R_P(M_\psi, r, \mu_r) - \frac{\alpha_s}{4\pi} \frac{1}{C_A} \frac{\pi^2}{\Delta} \right) \delta(1-\bar{z}) \right. \\ & + \frac{\alpha_s}{4\pi} \left[\left(4C_A \ln \frac{\left(\sqrt{(r+1)^2 \bar{z}^2 - 4r} + r\bar{z} - 2r + \bar{z} \right)^2}{4r(r+1)} - P[r, \bar{z}] (4C_A + \beta_0) \right) \right. \\ & \left. \left. \times \left[\frac{1}{1-\bar{z}} \right]_+ - 4C_A \left[\frac{\ln(1-\bar{z})}{1-\bar{z}} \right]_+ + P[r, \bar{z}] \mathcal{R}_P(\bar{z}, M_\psi, r, \mu_r) \right] \right\} + \mathcal{O}(\Delta), \end{aligned} \quad (3.26b)$$

where

$$\sigma_S^0 = \frac{64\pi^2 \alpha^2 \alpha_s e_c^2}{3s^2 M_\psi} \frac{1-r}{1+r}, \quad \sigma_P^0 = \frac{256\pi^2 \alpha^2 \alpha_s e_c^2}{27s^2 M_\psi^3} \frac{3+2r+7r^2}{(1-r)(1+r)}, \quad (3.27)$$

μ_r is the renormalization scale and the function $P[r, \bar{z}]$ is defined as

$$P[r, \bar{z}] = \frac{\sqrt{(1+r)^2 \bar{z}^2 - 4r}}{1-r}. \quad (3.28)$$

The expressions of R_S , R_P , \mathcal{R}_S and \mathcal{R}_P are listed in appendix A. Our analytical result for the S-wave differential cross section is equivalent to that in [54], and the analytical result for the P-wave channel is new.

3.3 Matching the short-distance hard parts

By inserting eqs. (3.17), (A.1), (3.26), (3.1) into the matching relation eq. (2.16) and using eq. (2.18), we can derive the short-distance hard parts $H^{(0)}$ directly. At LO we have

$$H_{[1S_0^{[8]}]}^{(0),LO}(z, M_\psi, s, x_{\min}, \mu_f) = \frac{64\pi^2 \alpha^2 \alpha_s e_c^2}{3s^2 M_\psi} \frac{1-r}{1+r} \delta(1-\bar{z}), \quad (3.29a)$$

$$H_{[3P^{[8]}]}^{(0),LO}(z, M_\psi, s, x_{\min}, \mu_f) = \frac{256\pi^2 \alpha^2 \alpha_s e_c^2}{27s^2 M_\psi^3} \frac{3+2r+7r^2}{(1-r)(1+r)} \delta(1-\bar{z}). \quad (3.29b)$$

One can find the short-distance hard part in P-wave channel is plagued with a singularity associated with the limit $r = M_\psi^2/s \rightarrow 1$. Inserting the above hard parts into the SGF formula, M_ψ will be replaced by M_ψ/x , and thus such singularity appears at the threshold limit $M_{c\bar{c}}^2 = M_\psi^2/x^2 \rightarrow s$, or $x \rightarrow \sqrt{r}$. In the threshold limit, the emitted gluon at LO

in figure 1 is very soft and its effect should be included in nonperturbative SGDs rather than in short-distance hard part. In fact, in the threshold region, ${}^3S_1^{[1]}$ channel can also contribute via $e^+e^- \rightarrow \gamma^* \rightarrow c\bar{c}({}^3S_1^{[1]})$, followed by the hadronization process described by the SGD $F_{[{}^3S_1^{[1]}] \rightarrow \psi}$. When ${}^3S_1^{[1]}$ channel is included, the matching process to determine the ${}^3P^{[8]}$ coefficient will have a contribution from the perturbative transition $F_{[{}^3S_1^{[1]}] \rightarrow c\bar{c}[{}^3P^{[8]}]}$, which will cancel the aforementioned threshold singularity.

However, in this paper we will be only interested in B-factories where $r \approx 0.1$ is very small. Then, when $x \sim \sqrt{r}$, the nonperturbative quantities SGDs have significant perturbatively calculable effects, which can be avoided by introducing a reasonable x_{\min} . By choosing $x_{\min} > \sqrt{r}$, both the contribution from $e^+e^- \rightarrow \gamma^* \rightarrow c\bar{c}({}^3S_1^{[1]})$ and the threshold singularity of P-wave channel will disappear. This is consistent with the fact that SGF formula is insensitive to small x_{\min} .

At NLO, we have

$$H_{[1S_0^{[8]}]}^{(0),NLO}(z, M_\psi, s, x_{\min}, \mu_f) = \left[\frac{d\sigma_S^{NLO}}{dz} - \int_{\max[\frac{\sqrt{z^2-4r+z}}{2}, x_{\min}]}^1 \frac{dx}{x} \frac{256\pi^2 \alpha^2 \alpha_s e_c^2 m_c^2 \mathcal{T}_x^2 x^3}{3s^2 M_\psi^3} \right. \\ \left. \times \left(1 - \frac{r}{x^2}\right) \delta(1 + r/x^2 - z/x) F_{[1S_0^{[8]}] \rightarrow c\bar{c}[1S_0^{[8]}]}^{NLO}(x, M_\psi, m_c, \mu_f) \right] \Big|_{m_c=M_\psi/2}, \quad (3.30)$$

where $\mathcal{T}_x = \mathcal{T}|_{M_\psi \rightarrow M_\psi/x}$. By integrating over x , we then obtain

$$H_{[1S_0^{[8]}]}^{(0),NLO}(z, M_\psi, s, x_{\min}, \mu_f) = \frac{\sigma_S^0 \alpha_s}{4\pi} \left\{ \left(R_S(M_\psi, r, \mu_r) + C_A \left(\ln^2 \frac{\mu_f^2 e^{-1}}{M_\psi^2} + \frac{\pi^2}{6} - 1 \right) \right) \right. \\ \times \delta(1 - \bar{z}) + \left(4C_A \ln \frac{\left(\sqrt{(r+1)^2 \bar{z}^2 - 4r} + r\bar{z} - 2r + \bar{z} \right)^2}{4r(r+1)} - P[r, \bar{z}] (4C_A + \beta_0) \right) \\ \times \left[\frac{1}{1 - \bar{z}} \right]_+ - 4C_A \left[\frac{\ln(1 - \bar{z})}{1 - \bar{z}} \right]_+ + P[r, \bar{z}] \mathcal{R}_S(\bar{z}, M_\psi, r, \mu_r) - \theta \left(z \geq \frac{x_{\min}^2 + r}{x_{\min}} \right) \\ \left. \times \frac{z(1+r)x_1^4 \mathcal{T}'^2 C_A}{(1-r)(x_1^2+r)} \left[\frac{4x_1}{(1-x_1)_+} \ln \left(\frac{x_1^2 \mu_f^2 e^{-1}}{M_\psi^2} \right) - 8x_1 \left(\frac{\ln(1-x_1)}{1-x_1} \right)_+ \right] \right\}, \quad (3.31)$$

with $\theta(t) = 0$ (1) if t is false (true), and

$$\mathcal{T}' = \frac{1}{2\sqrt{1-x_1^2}} \ln \frac{1 + \sqrt{1-x_1^2}}{1 - \sqrt{1-x_1^2}}, \quad (3.32a)$$

$$x_1 = \frac{\sqrt{z^2-4r+z}}{2}. \quad (3.32b)$$

We can find the above result still contains large logarithms at the limit $z \rightarrow 1+r$. These remained large logarithms originate from the collinear radiations recoil against the $c\bar{c}$ pair in the threshold region, which are not factorized in pure SGF. They can be resummed by introduce a jet function, as we will explain later.

Similarly, for the P-wave contribution we have

$$H_{[{}^3P^{[8]}]}^{(0),NLO}(z, M_\psi, s, x_{\min}, \mu_f) = \frac{\sigma_P^0 \alpha_s}{4\pi} \left\{ \left(R_P(M_\psi, r, \mu_r) + C_A \left(\ln^2 \frac{\mu_f^2 e^{-1}}{M_\psi^2} + \frac{\pi^2}{6} - 1 \right) \right) \right.$$

$$\begin{aligned}
& \times \delta(1 - \bar{z}) + \left(4C_A \ln \frac{\left(\sqrt{(r+1)^2 \bar{z}^2 - 4r} + r\bar{z} - 2r + \bar{z} \right)^2}{4r(r+1)} - P[r, \bar{z}](4C_A + \beta_0) \right) \\
& \times \left[\frac{1}{1 - \bar{z}} \right]_+ - 4C_A \left[\frac{\ln(1 - \bar{z})}{1 - \bar{z}} \right]_+ + P[r, \bar{z}] \mathcal{R}_P(\bar{z}, M_\psi, r, \mu_r) - \theta \left(z \geq \frac{x_{\min}^2 + r}{x_{\min}} \right) \\
& \times \frac{z \Theta(x_1, r) C_A}{z^2 - 4r} \left[\frac{4x_1}{(1 - x_1)_+} \ln \left(\frac{x_1^2 \mu_f^2 e^{-1}}{M_\psi^2} \right) - 8x_1 \left(\frac{\ln(1 - x_1)}{1 - x_1} \right)_+ \right] \Bigg\}, \quad (3.33)
\end{aligned}$$

with

$$\begin{aligned}
\Theta(x_1, r) = & \frac{(1 - r^2)x_1^2}{4(7r^2 + 2r + 3)(x_1 - 1)^2(x_1 + 1)^4(x_1^2 + r)} \left[r^2 \left(27\mathcal{T}'^2 x_1^8 + 72\mathcal{T}'^2 x_1^7 \right. \right. \\
& + (72\mathcal{T}'^2 - 264\mathcal{T}' + 79)x_1^4 + 24(3\mathcal{T}'^2 - 11\mathcal{T}' + 7)x_1^3 \\
& + 2(18\mathcal{T}'^2 - 60\mathcal{T}' + 65)x_1^2 + 6\mathcal{T}'(15\mathcal{T}' - 11)x_1^6 + 24\mathcal{T}'(3\mathcal{T}' - 7)x_1^5 \\
& \left. + 48x_1 + 16 \right) + 4r(x_1 - 1)x_1^2 \left(27\mathcal{T}'^2 x_1^4 + 4(9\mathcal{T}'^2 - 9\mathcal{T}' + 2)x_1^3 \right. \\
& + 2(9\mathcal{T}'^2 - 9\mathcal{T}' - 11)x_1^2 + 6\mathcal{T}'(3\mathcal{T}' - 1)x_1^5 + (6\mathcal{T}' - 26)x_1 - 5 \Big) \\
& + 6x_1^4 \left(3\mathcal{T}'^2 x_1^6 + 6\mathcal{T}'^2 x_1^5 + 2(3\mathcal{T}'^2 - 5\mathcal{T}' + 1)x_1^4 + (6\mathcal{T}'^2 - 20\mathcal{T}' + 9)x_1^2 \right. \\
& \left. \left. + (4 - 16\mathcal{T}')x_1^3 + (4\mathcal{T}' + 2)x_1 + 4 \right) \right]. \quad (3.34)
\end{aligned}$$

We can find in the last line of eq. (3.33) that the singularity at $z \rightarrow 2\sqrt{r}$ is avoided due to the introduction of cut off $x_{\min} > \sqrt{r}$. As a result, the cross section $\sigma_{J/\psi}$ is x_{\min} dependent. However, as demonstrated in appendix B, for small and moderate x_{\min} , the x_{\min} dependence of $\sigma_{J/\psi}$ is either α_s suppressed or $\Lambda_{\text{QCD}}/M_\psi$ suppressed. Thus the cross section $\sigma_{J/\psi}$ in SGF is insensitive to the choice of x_{\min} .

Inserting eqs. (3.29), (3.31) and (3.33) into eq. (2.17), we then obtain the differential cross section at the lowest order in the velocity expansion

$$\begin{aligned}
\frac{d\sigma_{J/\psi}}{dz} = & \int_{\max[(z + \sqrt{z^2 - 4r})/2, x_{\min}] }^1 \frac{dx}{x} \left[H_{[1S_0^{[8]}]}^{(0)}(\hat{z}, M_\psi/x, s, x_{\min}/x, \mu_f) F_{[1S_0^{[8]}] \rightarrow \psi}(x, M_\psi, m_c, \mu_f) \right. \\
& \left. + \sum_{J, \lambda} H_{[3P^{[8]}]}^{(0)}(\hat{z}, M_\psi/x, s, x_{\min}/x, \mu_f) F_{[3P_{J, \lambda}^{[8]}] \rightarrow \psi}(x, M_\psi, m_c, \mu_f) \right]. \quad (3.35)
\end{aligned}$$

4 NRQCD factorization

As a comparison, we also present here the results of NRQCD factorization. The CO contribution for inclusive J/ψ production can be factorized as

$$d\sigma(e^+e^- \rightarrow J/\psi + X) = d\hat{\sigma}[1S_0^{[8]}] \langle \mathcal{O}^{J/\psi}(1S_0^{[8]}) \rangle + \frac{1}{9} d\hat{\sigma}[3P^{[8]}] \langle \mathcal{O}^{J/\psi}(3P^{[8]}) \rangle, \quad (4.1)$$

where the factor 1/9 is to average over polarizations of intermediate states, and $\langle \mathcal{O}^{J/\psi}(3P^{[8]}) \rangle$ is the polarization-summed LDME defined by

$$\langle \mathcal{O}^{J/\psi}(3P^{[8]}) \rangle = \sum_{J, \lambda} \langle \mathcal{O}^{J/\psi}(3P_{J, \lambda}^{[8]}) \rangle, \quad (4.2)$$

which has following relation at the lowest order in velocity approximation,

$$\langle \mathcal{O}^{J/\psi}({}^3P^{[8]}) \rangle \approx 9 \langle \mathcal{O}^{J/\psi}[{}^3P_0^{[8]}] \rangle. \quad (4.3)$$

Based on perturbative differential cross sections calculated in section. 3.2, we can easily obtain the SDCs for NRQCD factorization

$$\begin{aligned} \frac{d\hat{\sigma}[{}^1S_0^{[8]}]}{dz} &= \sigma_S^{\prime 0} \left\{ \left(1 + \frac{\alpha_s}{4\pi} R_S(2m_c, r', \mu_r) \right) \delta(1-z') \right. \\ &+ \frac{\alpha_s}{4\pi} \left[\left(4C_A \ln \frac{\left(\sqrt{(r'+1)^2 z'^2 - 4r' + r'z' - 2r' + z'} \right)^2}{4r'(r'+1)} - P[r', z'](4C_A + \beta_0) \right) \right. \\ &\times \left. \left[\frac{1}{1-z'} \right]_+ - 4C_A \left[\frac{\ln(1-z')}{1-z'} \right]_+ + P[r', z'] \mathcal{R}_S(z', 2m_c, r', \mu_r) \right] \left. \right\} + \mathcal{O}(\alpha_s^3), \quad (4.4a) \end{aligned}$$

$$\begin{aligned} \frac{d\hat{\sigma}[{}^3P^{[8]}]}{dz} &= \sigma_P^{\prime 0} \left\{ \left(1 + \frac{\alpha_s}{4\pi} R_P(2m_c, r', \mu_r) \right) \delta(1-z') \right. \\ &+ \frac{\alpha_s}{4\pi} \left[\left(4C_A \ln \frac{\left(\sqrt{(r'+1)^2 z'^2 - 4r' + r'z' - 2r' + z'} \right)^2}{4r'(r'+1)} - P[r', z'](4C_A + \beta_0) \right) \right. \\ &\times \left. \left[\frac{1}{1-z'} \right]_+ - 4C_A \left[\frac{\ln(1-z')}{1-z'} \right]_+ + P[r', z'] \mathcal{R}_P(z', 2m_c, r', \mu_r) \right] \left. \right\} + \mathcal{O}(\alpha_s^3), \quad (4.4b) \end{aligned}$$

where

$$r' = \frac{4m_c^2}{s}, \quad z' = \frac{z}{1+r'}, \quad (4.5)$$

and

$$\sigma_S^{\prime 0} = \frac{32\pi^2 \alpha^2 \alpha_s e_c^2}{3s^2 m_c} \frac{1-r'}{1+r'}, \quad \sigma_P^{\prime 0} = \frac{32\pi^2 \alpha^2 \alpha_s e_c^2}{3s^2 m_c^3} \frac{3+2r'+7r'^2}{(1-r')(1+r')}. \quad (4.6)$$

Using the same multi-loop calculation techniques, we can also obtain integrated cross sections. The corresponding SDCs are given by

$$\hat{\sigma}[{}^1S_0^{[8]}] = (1+r') \sigma_S^{\prime 0} \left(1 + \frac{\alpha_s}{4\pi} \mathcal{G}_S(2m_c, r', \mu_r) \right) + \mathcal{O}(\alpha_s^3), \quad (4.7a)$$

$$\hat{\sigma}[{}^3P^{[8]}] = (1+r') \sigma_P^{\prime 0} \left(1 + \frac{\alpha_s}{4\pi} \mathcal{G}_P(2m_c, r', \mu_r) \right) + \mathcal{O}(\alpha_s^3), \quad (4.7b)$$

where \mathcal{G}_S and \mathcal{G}_P are given in appendix A. Our results can reproduce that in ref. [24] if we choose the same parameters therein.

Clearly, at the endpoint region, $z \rightarrow 1+r'$ (i.e. $z' \rightarrow 1$), the fixed-order results of the SDCs in eq. (4.4) suffer from large threshold logarithms. In order not to spoil the convergence of perturbative expansion, these threshold logarithms have to be resummed to all orders. Such resummation of the threshold logarithms to LO+NLL accuracy has been studied in ref. [26] within the SCET framework. According to [26, 54], at the endpoint region we have following factorization formula

$$\left. \frac{d\hat{\sigma}[n]}{dz'} \right|_{\text{endpoint}} = P[r', z'] (1+r') \sigma_{[n]}^{\prime 0} \mathcal{H}^{[n]}(\mu_r, \mu) \int_{z'}^1 d\xi \mathcal{S}^{[n]}(1-\xi, \mu) \mathcal{J}(s(1+r)(\xi-z'), \mu), \quad (4.8)$$

where a phase space factor $P[r', z']$ is introduced [26] with $P[r', 1] = 1$. Fixed-order expression of the SDCs at the endpoint can be read from eq. (4.4),

$$\begin{aligned} \left. \frac{d\hat{\sigma}[n]}{dz'} \right|_{\text{endpoint}} &= P[r', z'](1+r')\sigma_{[n]}^0 \left\{ \left(1 + \frac{\alpha_s}{4\pi} R_{[n]}(2m_c, r', \mu_r) \right) \delta(1-z') \right. \\ &\quad \left. + \frac{\alpha_s}{4\pi} \left[\left(4C_A \ln \frac{(1-r')^2}{r'(1+r')} - 4C_A - \beta_0 \right) \left(\frac{1}{1-z'} \right)_+ - 4C_A \left(\frac{\ln(1-z')}{1-z'} \right)_+ \right] \right\} + \mathcal{O}(\alpha_s^3). \end{aligned} \quad (4.9)$$

The shape function $\mathcal{S}^{[n]}(\xi)$ are defined in terms of ultrasoft fields that carry $\mathcal{O}(\Lambda_{\text{QCD}})$ momentum

$$\mathcal{S}^{[1S_0^{[8]}]}(1-\xi, \mu) = \frac{\langle 0 | \chi^\dagger T^a \psi a_\psi^\dagger a_\psi \delta((1-\xi) + i\hat{l} \cdot D) \psi^\dagger T^a \chi | 0 \rangle}{4m_c \langle \mathcal{O}^{J/\psi} [1S_0^{[8]}] \rangle}, \quad (4.10a)$$

$$\mathcal{S}^{[3P_0^{[8]}]}(1-\xi, \mu) = \frac{\frac{1}{3} \langle 0 | \chi^\dagger \left(-\frac{i}{2} \overleftrightarrow{\mathbf{D}} \cdot \boldsymbol{\sigma} \right) T^a \psi a_\psi^\dagger a_\psi \delta((1-\xi) + i\hat{l} \cdot D) \psi^\dagger \left(-\frac{i}{2} \overleftrightarrow{\mathbf{D}} \cdot \boldsymbol{\sigma} \right) T^a \chi | 0 \rangle}{4m_c \langle \mathcal{O}^{J/\psi} [3P_0^{[8]}] \rangle}, \quad (4.10b)$$

where the ultrasoft covariant derivative is given as $D^\mu = \partial^\mu - ig_s A_{us}^\mu$, the lightlike vector \hat{l}^μ is defined as $\hat{l}^\mu = \sqrt{2}l^\mu/M_S$ with $M_S \equiv 2m_c(1+r)/(1-r)$, and ψ and χ denote the Pauli spinor fields in NRQCD that annihilates a heavy quark and creates a heavy antiquark, respectively. The jet function describes the collinear radiations recoil against the J/ψ in the threshold region, which is defined as

$$\mathcal{J}(p^2, \mu) = -\frac{s(1+r)}{4\pi} \text{Im} \left[i \int d^4y e^{ip \cdot y} \langle 0 | T \left(\text{Tr}[T^a B_\perp^{(0)\beta}(y)] \text{Tr}[T^a B_{\perp\beta}^{(0)}(0)] \right) | 0 \rangle \right], \quad (4.11)$$

where the superscript (0) denotes the bare field, B_\perp^μ is the collinear gauge invariant effective field [26], and the factor $s(1+r)$ is chosen to provide a convenient normalization for the process considered here. According to [55, 56], the fixed-order expression of the shape function and jet function are given by

$$\begin{aligned} \mathcal{S}^{[n]}(1-\xi, \mu) &= \delta(1-\xi) + \frac{\alpha_s C_A}{4\pi} \left[\frac{4}{(1-\xi)_+} \ln \left(\frac{\mu^2 e^{-1}}{M_S^2} \right) - 8 \left(\frac{\ln(1-\xi)}{1-\xi} \right)_+ \right. \\ &\quad \left. - \delta(1-x) \left(\ln^2 \left(\frac{\mu^2 e^{-1}}{M_S^2} \right) + \frac{\pi^2}{6} - 1 \right) \right] + \mathcal{O}(\alpha_s^2), \end{aligned} \quad (4.12a)$$

$$\begin{aligned} \mathcal{J}(M_J^2(\xi-z'), \mu) &= \delta(\xi-z') + \frac{\alpha_s}{4\pi} \left\{ \left[C_A \left(\frac{67}{9} - \pi^2 \right) - \frac{20}{9} T_f n_f - \beta_0 \ln \frac{M_J^2}{\mu^2} \right. \right. \\ &\quad \left. \left. + 2C_A \ln^2 \frac{M_J^2}{\mu^2} \right] \delta(\xi-z') + \left(4C_A \ln \frac{M_J^2}{\mu^2} - \beta_0 \right) \left[\frac{1}{\xi-z'} \right]_+ \right. \\ &\quad \left. + 4C_A \left[\frac{\ln(\xi-z')}{\xi-z'} \right]_+ \right\} + \mathcal{O}(\alpha_s^2), \end{aligned} \quad (4.12b)$$

where $M_J^2 \equiv s(1+r)$.

Similar to SGF, to perform the resummation of the factorization formula eq. (4.8), we transform it to Laplace space

$$\begin{aligned}
\bar{\sigma}[n](\nu) &= \int_0^\infty d\omega e^{-\nu\omega} \frac{1}{P[r', z']} \left. \frac{d\hat{\sigma}[n]}{dz'} \right|_{\text{endpoint}} \\
&= (1+r')\sigma_{[n]}^0 \mathcal{H}^{[n]}(\mu_r, \mu) \int_0^\infty d\omega e^{-\nu\omega} \int_0^\omega d\omega' \mathcal{S}^{[n]}(\omega', \mu) \mathcal{J}(M_J^2(\omega - \omega'), \mu) \\
&= (1+r')\sigma_{[n]}^0 \mathcal{H}^{[n]}(\mu_r, \mu) \tilde{\mathcal{S}}^{[n]}(\nu, \mu) \tilde{\mathcal{J}}(\nu, \mu), \tag{4.13}
\end{aligned}$$

where we introduce $\omega = 1 - z'$ and $\omega' = 1 - \xi$, with ω' denoting the longitudinal momentum fraction of the emitted ultrasoft gluons in the shape function. Different from the momentum fraction $\omega_0 = (1-x)/x$ in SGD, which takes values between 0 and ∞ , ω' takes values between 0 and 1. Actually, the exact form of ω' should be $\omega' = (1 - \xi)/\xi$, which also runs from 0 to ∞ . However, in NRQCD+SCET approach one only consider the resummation in the endpoint region ($\xi \rightarrow 1$), where one has $\omega' = (1 - \xi)/\xi \sim 1 - \xi$, i.e. the evolution of the terms at higher order in $1 - \xi$ is not included. While in the evolution of SGD, these contributions are included. In eq. (4.13), $\tilde{\mathcal{S}}^{[n]}(\nu, \mu)$ and $\tilde{\mathcal{J}}(\nu, \mu)$ are the Laplace transformation of shape function and jet function,

$$\tilde{\mathcal{S}}^{[n]}(\nu, \mu) = \int_0^\infty d\omega' e^{-\nu\omega'} \mathcal{S}^{[n]}(\omega', \mu), \tag{4.14a}$$

$$\tilde{\mathcal{J}}(\nu, \mu) = \int_0^\infty d\omega' e^{-\nu\omega'} \mathcal{J}(M_J^2\omega', \mu). \tag{4.14b}$$

The components $\tilde{\mathcal{S}}^{[n]}$, $\tilde{\mathcal{J}}$ and $\mathcal{H}^{[n]}$ satisfy the renormalization group equations

$$\frac{d\tilde{\mathcal{S}}^{[n]}(\nu, \mu)}{d \ln \mu} = \left[-2\Gamma_{\text{cusp}}^S(\alpha_s) \ln \frac{\bar{\nu}\mu}{M_S} + \gamma^S(\alpha_s) \right] \tilde{\mathcal{S}}^{[n]}(\nu, \mu), \tag{4.15a}$$

$$\frac{d\tilde{\mathcal{J}}(\nu, \mu)}{d \ln \mu} = \left[-2\Gamma_{\text{cusp}}^J(\alpha_s) \ln \frac{\bar{\nu}\mu^2}{M_J^2} + \gamma^J(\alpha_s) \right] \tilde{\mathcal{J}}(\nu, \mu), \tag{4.15b}$$

$$\frac{d\mathcal{H}^{[n]}(\mu_r, \mu)}{d \ln \mu} = \left[-2\Gamma_{\text{cusp}}^H(\alpha_s) \ln \frac{\mu M_S}{M_J^2} + \gamma^H(\alpha_s) \right] \mathcal{H}^{[n]}(\mu_r, \mu), \tag{4.15c}$$

where anomalous dimensions obey relations $\Gamma_{\text{cusp}}^S = -\Gamma_{\text{cusp}}^J = \Gamma_{\text{cusp}}^H$ and $\gamma^S + \gamma^J + \gamma^H = 0$, and they are universal series in α_s ,

$$\begin{aligned}
\Gamma_{\text{cusp}}^K(\alpha_s) &= \sum_{m=0} \left(\frac{\alpha_s}{4\pi} \right)^{m+1} \Gamma_m^K, \\
\gamma^K(\alpha_s) &= \sum_{m=0} \left(\frac{\alpha_s}{4\pi} \right)^{m+1} \gamma_m^K, \quad K = S, J, H. \tag{4.16}
\end{aligned}$$

Up to NLL accuracy, the needed coefficients are [26, 57]

$$\begin{aligned}
\Gamma_0^S &= -\Gamma_0^J = \Gamma_0^H = 4C_A, \\
\Gamma_1^S &= -\Gamma_1^J = \Gamma_1^H = 4C_A \left[\left(\frac{67}{9} - \frac{\pi^2}{3} \right) C_A - \frac{20}{9} T_f n_f \right],
\end{aligned}$$

$$\begin{aligned}
\gamma_0^S &= 4C_A, \\
\gamma_0^J &= 2\beta_0, \\
\gamma_0^H &= -4C_A - 2\beta_0.
\end{aligned} \tag{4.17}$$

We choose characteristic scales for $\mathcal{H}^{[n]}$, $\mathcal{S}^{[n]}$ and \mathcal{J} as follow

$$\mu_H = \mu_r, \tag{4.18a}$$

$$\mu_S = \frac{\mu_r}{\nu}, \tag{4.18b}$$

$$\mu_J = \sqrt{\mu_H \mu_S} = \frac{\mu_r}{\sqrt{\nu}}, \tag{4.18c}$$

then by solving the RGEs in eq. (4.15), we can evolve these functions from their characteristic scales to the scale μ_r . Therefore, we get the resummed result

$$\tilde{\sigma}[n](\nu)|_{\text{resummed}} = (1 + r')\sigma_{[n]}^0 \mathcal{H}^{[n]}(\mu_r, \mu_r) \tilde{\mathcal{S}}^{[n]}(\nu, \mu_r/\nu) \tilde{\mathcal{J}}(\nu, \mu_r/\sqrt{\nu}) \exp[h(\mu_r, \chi_1, \chi_2)], \tag{4.19}$$

where

$$\begin{aligned}
\mathcal{H}^{[n]}(\mu_r, \mu_r) \tilde{\mathcal{S}}^{[n]}(\nu, \mu_r/\nu) \tilde{\mathcal{J}}(\nu, \mu_r/\sqrt{\nu}) &= 1 + \frac{\alpha_s}{4\pi} R_{[n]}(2m_c, r', \mu_r) + \frac{\alpha_s}{4\pi} \left(-2C_A \gamma_E^2 \right. \\
&\quad \left. - 8C_A \gamma_E \ln \frac{M_J}{M_S} + (4C_A + \beta_0) \gamma_E - \frac{\pi^2}{3} C_A \right) + \mathcal{O}(\alpha_s^2),
\end{aligned} \tag{4.20}$$

and the evolution function is given by

$$\begin{aligned}
h(\mu_r, \chi_1, \chi_2) &= \frac{2\pi\Gamma_0^S}{\beta_0^2} \frac{1}{\alpha_s(\mu_r)} \left((2\chi_1 - 1) \ln(1 - 2\chi_1) - 2(\chi_2 - 1) \ln(1 - \chi_2) \right) \\
&\quad + \frac{\Gamma_0^S}{\beta_0} \left[\ln(1 - 2\chi_1) \ln\left(\frac{\mu_r e^{\gamma_E}}{M_S}\right) - \ln(1 - \chi_2) \ln\left(\frac{\mu_r^2 e^{\gamma_E}}{M_J^2}\right) \right] \\
&\quad - \frac{1}{2\beta_0} \left(\gamma_0^J \ln(1 - \chi_2) + \gamma_0^S \ln(1 - 2\chi_1) \right) - \frac{\beta_1 \Gamma_0^S}{4\beta_0^3} \left(\ln^2(1 - 2\chi_1) - 2\ln^2(1 - \chi_2) \right) \\
&\quad + \frac{\Gamma_0^S}{2\beta_0^2} \left(\frac{\Gamma_1^S}{\Gamma_0^S} - \frac{\beta_1}{\beta_0} \right) \left(\ln(1 - 2\chi_1) - 2\ln(1 - \chi_2) \right),
\end{aligned} \tag{4.21}$$

with

$$\chi_1 = \chi_2 = \frac{\alpha_s(\mu_r)\beta_0}{4\pi} \ln \nu. \tag{4.22}$$

Similar to the SGD, to deal with the Landau singularity, we make following replacement in eq. (4.21)

$$\chi_1 \rightarrow \chi_{1*} = \frac{\alpha_s(\mu_r)\beta_0}{4\pi} \ln\left(\frac{\nu}{1 + \nu/\nu_{1*}^L}\right), \quad \nu_{1*}^L = \nu_1^L/a, \tag{4.23}$$

$$\chi_2 \rightarrow \chi_{2*} = \frac{\alpha_s(\mu_r)\beta_0}{4\pi} \ln\left(\frac{\nu}{1 + \nu/\nu_{2*}^L}\right), \quad \nu_{2*}^L = \nu_2^L/a, \tag{4.24}$$

with branch points ν_1^L and ν_2^L given by

$$\nu_1^L = \exp\left(\frac{2\pi}{\beta_0\alpha_s(\mu_r)}\right), \quad \nu_2^L = \exp\left(\frac{4\pi}{\beta_0\alpha_s(\mu_r)}\right). \quad (4.25)$$

The resummed cross section is modified as

$$\begin{aligned} \tilde{\sigma}[n](\nu)|_{\text{resummed}} = & (1+r')\sigma_{[n]}^0 \left[1 + \frac{\alpha_s}{4\pi} R_{[n]}(2m_c, r', \mu_r) + \frac{\alpha_s}{4\pi} \left(-2C_A\gamma_E^2 - 8C_A\gamma_E \ln \frac{M_J}{M_S} \right. \right. \\ & \left. \left. + (4C_A + \beta_0)\gamma_E - \frac{\pi^2}{3}C_A \right) \right] \exp[h(\mu_r, \chi_{1*}, \chi_{2*})] \tilde{\mathcal{S}}_{[n]}^{\text{mod}}(\nu). \end{aligned} \quad (4.26)$$

On the other hand, from eq. (4.9) we can derive the fixed-order expression of $\tilde{\sigma}[n](\nu)$ as

$$\begin{aligned} \tilde{\sigma}[n](\nu) = & (1+r')\sigma_{[n]}^0 \left\{ 1 + \frac{\alpha_s}{4\pi} R_{[n]}(2m_c, r', \mu_r) + \frac{\alpha_s}{4\pi} \left[\left(-8C_A \ln \frac{M_J}{M_S} + 4C_A + \beta_0 \right) \ln \bar{\nu} \right. \right. \\ & \left. \left. - 2C_A \left(\ln^2 \bar{\nu} + \frac{\pi^2}{6} \right) \right] \right\}. \end{aligned} \quad (4.27)$$

Comparing with eq. (4.26), we can find the single and double logarithms of ν in eq. (4.27) have been resummed. It should be noted that our choice of the characteristic scales in eq. (4.18) is different from that in refs. [26, 54]. Their scales choices not only resum the logarithms of ν , but also try to resum logarithms of $\ln(s/m_c^2)$. However, terms of $\ln(s/m_c^2)$ can only be resummed by using the double-parton fragmentation framework [58–61], which is beyond the scope of this paper.

Using the numerical Laplace inverse transformation, we then obtain the resummed cross section in momentum space as

$$\left. \frac{d\hat{\sigma}[n]}{dz'} \right|_{\text{resummed}} = \frac{1}{2\pi i} \int_{c-i\infty}^{c+i\infty} d\nu e^{(1-z')\nu} (\tilde{\sigma}[n](\nu)|_{\text{resummed}}). \quad (4.28)$$

Combining eqs. (4.28) and the SDCs results, we obtain the NLO+NLL results

$$\left. \frac{d\hat{\sigma}[n]}{dz} \right|_{\text{NLO+NLL}} = \left. \frac{d\hat{\sigma}[n]}{dz} \right|_{\text{resummed}} + \frac{P[r', z']}{1+r'} \left. \frac{d\hat{\sigma}[n]}{dz'} \right|_{\text{resummed}} - \frac{1}{1+r'} \left. \frac{d\hat{\sigma}[n]}{dz'} \right|_{\text{endpoint}}, \quad (4.29)$$

where the subtraction of the last term is to avoid double counting between the endpoint and the full z range.

As discussed before, in the pure SGF, only logarithms coming from soft gluon emission are resummed by using the RGEs of SGDs. And the evolution kernels for RGEs are known to $\mathcal{O}(\alpha_s)$. For a comparison, here we also give two partly resummed results in NRQCD+SCET framework, which we denote as \mathcal{S} -resum cross section and \mathcal{J} -resum cross section. In deriving the \mathcal{S} -resum cross section, the evolution of jet function is closed by choosing initial scales as

$$\mu_H = \mu_r, \quad \mu_S = \frac{\mu_r}{\nu}, \quad \mu_J = \mu_r. \quad (4.30)$$

Similarly, for \mathcal{J} -resum cross section, the evolution of shape function is closed by following initial scales choice

$$\mu_H = \mu_r, \quad \mu_S = \mu_r, \quad \mu_J = \frac{\mu_r}{\sqrt{\nu}}. \quad (4.31)$$

In addition, in these two cases we only include the $\mathcal{O}(\alpha_s)$ terms of the anomalous dimensions in eq. (4.16). Then these two partly resummed cross sections read

$$\begin{aligned} \tilde{\sigma}[n](\nu) \Big|_{\mathcal{S}\text{-resum}} &= (1+r')\sigma_{[n]}^{\prime 0} \left[1 + \frac{\alpha_s}{4\pi} R_{[n]}(2m_c, r', \mu_r) + \frac{\alpha_s}{4\pi} \left(\beta_0 \ln \bar{\nu} + 2C_A \ln^2 \bar{\nu} \right. \right. \\ &\quad \left. \left. - 8C_A \ln \bar{\nu} \ln \frac{M_J}{\mu_r} - 8C_A \gamma_E \ln \frac{\mu_r}{M_S} - 4C_A \gamma_E^2 + 4C_A \gamma_E - \frac{\pi^2}{3} C_A \right) \right] \\ &\quad \times \exp [h_S(\mu_r, \chi_{1*})] \tilde{\mathcal{S}}_{[n]}^{\text{mod}}(\nu), \end{aligned} \quad (4.32a)$$

$$\begin{aligned} \tilde{\sigma}[n](\nu) \Big|_{\mathcal{J}\text{-resum}} &= (1+r')\sigma_{[n]}^{\prime 0} \left[1 + \frac{\alpha_s}{4\pi} R_{[n]}(2m_c, r', \mu_r) + \frac{\alpha_s}{4\pi} \left(4C_A \gamma_E \ln \frac{M_S^2}{M_J^2} + \beta_0 \gamma_E \right. \right. \\ &\quad \left. \left. + 4C_A \ln \bar{\nu} - 2C_A \ln^2 \bar{\nu} - 2C_A \ln^2 \nu + 4C_A \ln \frac{M_S^2}{\mu_r^2 e^{\gamma_E}} \ln \nu - \frac{\pi^2}{3} C_A \right) \right] \\ &\quad \times \exp [h_J(\mu_r, \chi_{2*})] \tilde{\mathcal{S}}_{[n]}^{\text{mod}}(\nu), \end{aligned} \quad (4.32b)$$

with

$$\begin{aligned} h_S(\mu_r, \chi_{1*}) &= \frac{2\pi\Gamma_0^S}{\beta_0^2} \frac{1}{\alpha_s(\mu_r)} \left(- (1 - 2\chi_{1*}) \ln(1 - 2\chi_{1*}) - 2\chi_{1*} \right) - \frac{\gamma_0^S}{2\beta_0} \ln(1 - 2\chi_{1*}) \\ &\quad + \frac{\Gamma_0^S}{\beta_0} \ln(1 - 2\chi_{1*}) \ln \frac{\mu_r e^{\gamma_E}}{M_S}, \end{aligned} \quad (4.33a)$$

$$\begin{aligned} h_J(\mu_r, \chi_{2*}) &= \frac{2\pi\Gamma_0^S}{\beta_0^2} \frac{1}{\alpha_s(\mu_r)} \left(2(1 - \chi_{2*}) \ln(1 - \chi_{2*}) + 2\chi_{2*} \right) - \frac{\gamma_0^J}{2\beta_0} \ln(1 - \chi_{2*}) \\ &\quad - \frac{\Gamma_0^S}{\beta_0} \ln(1 - \chi_{2*}) \ln \frac{\mu_r^2 e^{\gamma_E}}{M_J^2}. \end{aligned} \quad (4.33b)$$

And the results in momentum space are

$$\frac{d\hat{\sigma}[n]}{dz'} \Big|_{\mathcal{S}\text{-resum}} = \frac{1}{2\pi i} \int_{c-i\infty}^{c+i\infty} d\nu e^{(1-z')\nu} (\tilde{\sigma}[n](\nu) \Big|_{\mathcal{S}\text{-resum}}), \quad (4.34a)$$

$$\frac{d\hat{\sigma}[n]}{dz'} \Big|_{\mathcal{J}\text{-resum}} = \frac{1}{2\pi i} \int_{c-i\infty}^{c+i\infty} d\nu e^{(1-z')\nu} (\tilde{\sigma}[n](\nu) \Big|_{\mathcal{J}\text{-resum}}). \quad (4.34b)$$

Finally we denote the partly resummed NLO results as

$$\frac{d\hat{\sigma}[n]}{dz} \Big|_{\mathcal{S}\text{-resum}} = \frac{d\hat{\sigma}[n]}{dz} + \frac{P[r', z']}{1+r'} \frac{d\hat{\sigma}[n]}{dz'} \Big|_{\mathcal{S}\text{-resum}} - \frac{1}{1+r'} \frac{d\hat{\sigma}[n]}{dz'} \Big|_{\text{endpoint}}, \quad (4.35a)$$

$$\frac{d\hat{\sigma}[n]}{dz} \Big|_{\mathcal{J}\text{-resum}} = \frac{d\hat{\sigma}[n]}{dz} + \frac{P[r', z']}{1+r'} \frac{d\hat{\sigma}[n]}{dz'} \Big|_{\mathcal{J}\text{-resum}} - \frac{1}{1+r'} \frac{d\hat{\sigma}[n]}{dz'} \Big|_{\text{endpoint}}. \quad (4.35b)$$

5 Phenomenology

In this section, we present phenomenological analysis based on our calculations in previous sections. The center-of-mass energy is chosen as $\sqrt{s} = 10.6\text{GeV}$ for B factories. The QED coupling constant is set as $\alpha = 1/137$. We determine the value of the coupling constant $\alpha_s(\mu_r)$ by adopting the two-loop RGE formula and setting $\Lambda_{\overline{\text{MS}}}^{(3)} = 388\text{MeV}$, and we set the renormalization scale $\mu_r = \sqrt{s}/2 = 5.3\text{GeV}$. We take the J/ψ mass $M_\psi = 3.1\text{GeV}$ and the heavy quark mass $m_c = 1.5\text{GeV}$. For nonperturbative model $\tilde{F}^{\text{mod}}[n](\nu)$ and $\tilde{S}_{[n]}^{\text{mod}}(\nu)$, we adopt the model function used in [26, 54, 55, 62], which in Laplace space are given by

$$\tilde{F}^{\text{mod}}[n](\nu) = N^\psi[n] \left(\frac{\nu\bar{\Lambda}}{AM_\psi} + 1 \right)^{-AB}, \quad (5.1a)$$

$$\tilde{S}_{[n]}^{\text{mod}}(\nu) = \left(\frac{\nu\bar{\Lambda}}{AM_S} + 1 \right)^{-AB}. \quad (5.1b)$$

Following ref. [26], we assume that the parameters A , B and $\bar{\Lambda}$ in the model functions are the same for both of the S-wave and P-wave contributions. Furthermore, we also assume that these parameters are the same for the models of SGDs and shape functions. We set $A = 1$, $B = 2$, $\bar{\Lambda} = 0.3\text{GeV}$ [26], $a = 1.1$ and $x_{\min} = 0.5$. $N^\psi[n]$ is the normalization of the model of SGD and we set [2]

$$N^\psi[1S_0^{[8]}] = \langle \mathcal{O}^{J/\psi}(1S_0^{[8]}) \rangle, \quad (5.2a)$$

$$N^\psi[3P_{J,\lambda}^{[8]}] = \langle \mathcal{O}^{J/\psi}(3P_0^{[8]}) \rangle. \quad (5.2b)$$

Then after integrating out x , both the differential cross sections in SGF approach and in NRQCD approach can be written in the form

$$d\sigma(e^+e^- \rightarrow J/\psi + X) = d\hat{\sigma}_S \langle \mathcal{O}^{J/\psi}(1S_0^{[8]}) \rangle + d\hat{\sigma}_P \langle \mathcal{O}^{J/\psi}(3P_0^{[8]}) \rangle. \quad (5.3)$$

And for the integrated cross sections we have

$$\sigma(e^+e^- \rightarrow J/\psi + X) = \hat{\sigma}_S \langle \mathcal{O}^{J/\psi}(1S_0^{[8]}) \rangle + \hat{\sigma}_P \langle \mathcal{O}^{J/\psi}(3P_0^{[8]}) \rangle. \quad (5.4)$$

In figure 3 we show the coefficients of the differential cross section in NRQCD factorization approach with different resummation methods. We can see that the resummed differential cross sections are much softer than the result in NRQCD factorization. Moreover, in the NLO+NLL case the unphysical enhancement near the endpoint is cured by taking the resummation and nonperturbative shape function model into account. But the existence of the next-to-leading power logarithms, like $\ln(1-z')$, which are not resummed, still drives the differential cross section divergent in the endpoint region. We also find the \mathcal{S} -resum cross section is close to the result in NLO+NLL method, while the \mathcal{J} -resum cross section is deviate from the NLO+NLL result seriously. This phenomenon indicates that, as a good approximation, it makes sense to neglect the evolution of the jet function, as was done in pure SGF.

In figure 4 we show the differential cross sections in SGF comparing with that in NRQCD factorization. Due to the introduction of x_{\min} , the z distribution in SGF approach

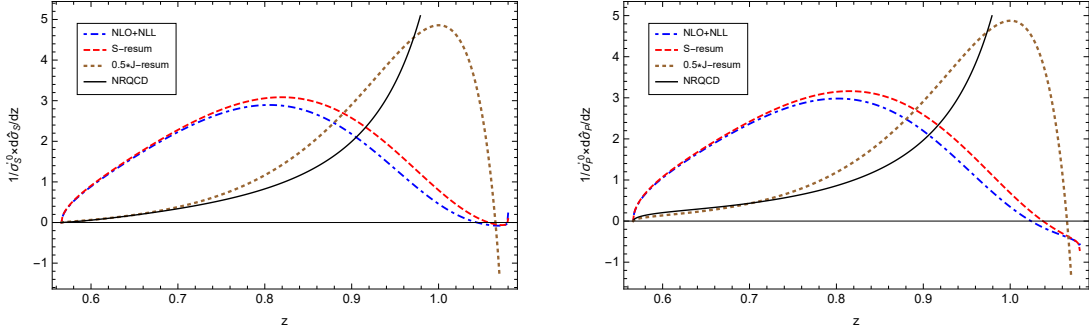


Figure 3. The differential cross section in NRQCD factorization approach with different resummation methods. Left figure is the S-wave contribution and right figure is the P-wave contribution. The \mathcal{J} -resum cross section is multiplied by a factor 0.5.

is piecewise function. Therefore, here we calculate the z distributions in 20 bins, and plot the average value for each bin. We find the peak in NRQCD+NLL results is on the left of that in SGF. We also find that, comparing to the NLO+NLL results, the SGF results are significantly suppressed at moderate z , especially for the P-wave case. There are many origins for these differences. First, in solving the RGEs of SGDs, we have included the effects at higher order in $1-x$, which will shift the peak to the right. While in the NRQCD+NLL method these effects have been ignored. Second, as shown in eqs.(3.29), (3.31) and (3.33), in SGF approach the hard parts in S-wave and P-wave are proportional to an overall factor x and x^3 (due to the factor $1/M_\psi$ and $1/M_\psi^3$) respectively, which originated from velocity corrections resummation. Such factors suppress the differential cross sections at moderate z , especially for the P-wave. This implies that, even though large logarithms are resummed in NRQCD+SCET approach, there are still significant velocity corrections. Resumming these velocity corrections is the main purpose of the SGF. Finally, the SGF results included partial contributions at order $\mathcal{O}(\alpha_s^3)$, which come from the convolution of NLO short-distance hard parts with the resummed SGDs.

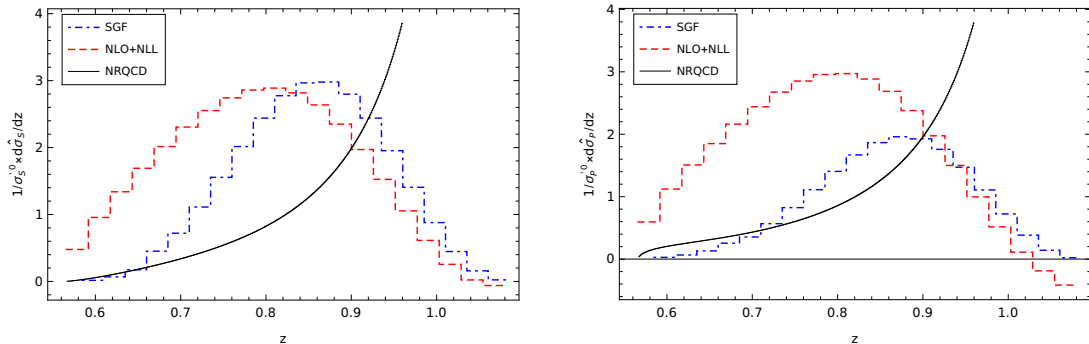


Figure 4. The differential cross sections in SGF and NRQCD factorization approaches.

In Table.1 we list the coefficients of the integrated cross section in different methods. We find the \mathcal{S} -resum results are close to the NLO+NLL results. Besides, both the NLO+NLL results and SGF results are much smaller than the NRQCD results due to resummation effects. Comparing to the NLO+NLL results, the SGF results are further suppressed.

	NRQCD	NLO+NLL	\mathcal{S} -resum	SGF
$\hat{\sigma}_S^{\text{NLO}}$ (pb/GeV ³)	17.677	7.411	8.246	5.986
$\hat{\sigma}_P^{\text{NLO}}$ (pb/GeV ⁵)	30.370	12.691	14.096	6.541

Table 1. The coefficients of the integrated cross section in different methods.

In figure 5 we show the x_{\min} dependence of the z distributions by varying x_{\min} from 0.4 to 0.55. We find different choices of x_{\min} can only slightly affect the distribution at moderate z as far as x_{\min} is not too large, e.g., $x_{\min} < 0.55$. In Table.2, x_{\min} dependence of coefficients of cross section is shown. We find differences are smaller than 2%, which confirms our argument in appendix B that the cross section $\sigma_{J/\psi}$ in SGF is not sensitive to the choice of x_{\min} .

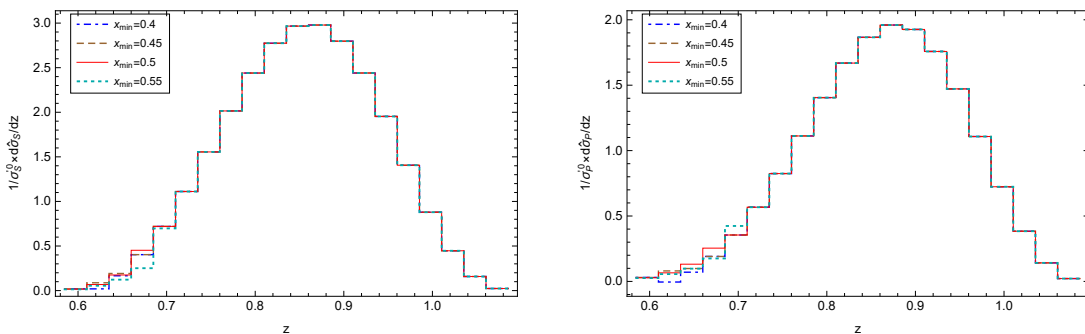


Figure 5. The differential cross sections in SGF with different x_{\min} .

	$x_{\min}=0.4$	$x_{\min}=0.45$	$x_{\min}=0.5$	$x_{\min}=0.55$
$\hat{\sigma}_S^{\text{NLO}}$ (pb/GeV ³)	5.963	5.984	5.986	5.922
$\hat{\sigma}_P^{\text{NLO}}$ (pb/GeV ⁵)	6.471	6.512	6.541	6.521

Table 2. The coefficients of the integrated cross section in SGF with different x_{\min} .

Following ref. [24], we define a linear combination of CO LDMEs as:

$$M_k^X = \langle \mathcal{O}^{J/\psi}(1S_0^{[8]}) \rangle + k \frac{\langle \mathcal{O}^{J/\psi}(3P_0^{[8]}) \rangle}{m_c^2}, \quad (5.5)$$

where “X” denotes factorization approach. If we set the CS contribution to be zero, and use the CO contribution to saturate the observed production cross section [9]

$$\sigma[e^+e^- \rightarrow J/\psi + X_{\text{non-}c\bar{c}}] = 0.43 \pm 0.13 \text{pb}, \quad (5.6)$$

we can get an upper bound for the CO matrix element in each approach. Using the coefficients in Table.1, we then obtain

$$M_{3.9}^{\text{NRQCD}} < (2.4 \pm 0.7) \times 10^{-2} \text{GeV}^3, \quad (5.7a)$$

$$M_{3.9}^{\text{NLO+NLL}} < (5.8 \pm 1.8) \times 10^{-2} \text{GeV}^3, \quad (5.7b)$$

$$M_{2.5}^{\text{SGF}} < (7.2 \pm 2.2) \times 10^{-2} \text{GeV}^3. \quad (5.7c)$$

On the other hand, the value of CO LDME M_k extracted from hadron colliders reads [28]

$$M_{3.9}^{\text{NRQCD,pp}} = (7.4 \pm 1.9) \times 10^{-2} \text{GeV}^3, \quad (5.8)$$

which is about 3 times larger than the upper bound of $M_{3.9}^{\text{NRQCD}}$. Such a large discrepancy challenges the universality of NRQCD LDMEs. The SGF approach significantly reduces this discrepancy, which provides a hope to solve the universality problem. To this end, we must also describe J/ψ production in hadron colliders using SGF, which will be studied in future works.

6 Summary

In summary, in this paper we studied the J/ψ production via color-octet channel, $e^+e^- \rightarrow J/\psi(3P_J^{[8]}, 1S_0^{[8]}) + X_{\text{non-}c\bar{c}}$, in SGF approach, in which a series of important velocity corrections can be resummed naturally. The corresponding J/ψ energy spectrum is expressed as a convolution of perturbatively calculable short-distance hard parts with one-dimensional color-octet SGDs, as shown in eq. (2.8). We introduced a cutoff x_{min} for the longitudinal momentum fraction of the emitted soft gluons to prevent the gluons to be hard. We demonstrated both analytically and numerically that the x_{min} dependence is suppressed and can be ignored in the sense of perturbation theory.

We calculated short-distance hard parts analytically up to NLO in α_s . We derived and solved RGEs of SGDs, which resums Sudakov logarithms originated from soft gluons emission. Then by adopting a simple model for SGDs at an initial scale, our results are well-behaved near the kinematic endpoint, and they have the same shape as experimental data for the energy spectrum. By ignoring color-singlet contribution and using color-octet contributions to saturate the observed production cross section $\sigma[e^+e^- \rightarrow J/\psi + X_{\text{non-}c\bar{c}}]$, we get an upper bound for the color-octet matrix element M_k^X , which seems to be consistent with the value extracted from hadron colliders.

However, there are two questions needing to be understood before we can convince ourselves that SGF has provided a reasonable description of J/ψ production. The first question is how important of the Sudakov logarithms originated from jet functions which have not been resummed in SGF. If this effect is very important, we need to do further job to resum them. The second question is how important of the velocity-correction terms that have been resummed in SGF. If this effect is not important, we do not really need the SGF approach, but simply using the NRQCD factorization combining with resummation methods to deal with Sudakov logarithms.

To understand the above two questions, we also calculated the same quantity in NRQCD factorization and use NRQCD+SCET approach to resum all encountered Sudakov logarithms. It was found that the full NRQCD+SCET result is very close to the result in which Sudakov logarithms originated from jet functions are not resummed. But if Sudakov logarithms originated from soft gluons emission are not resummed, one will get a result with large deviation from the full result. This answered the first question that Sudakov logarithms originated from jet functions are not that important. By comparing the NRQCD+SCET result with SGF result, we still find large difference, which implies that the resummation of velocity-correction terms is significant for phenomenological study.

With the understanding of the above two questions, we conclude that we have provided by far the best theoretical framework to describe J/ψ production in e^+e^- collisions. To further understand the production mechanism of quarkonium, it will be very useful to apply SGF for other processes, like photo- or hadroproduction, in the future.

7 Acknowledgments

We thank Kuang-Ta Chao and Xiaohui Liu for many useful discussion. The work is supported in part by the National Natural Science Foundation of China (Grants No. 11875071, No. 11975029), the National Key Research and Development Program of China under Contracts No. 2020YFA0406400.

A Analytic expressions

In this appendix, we provide analytic expressions of the functions $d\sigma_P^{LO}/dz$, R_S , R_P , \mathcal{R}_S , \mathcal{R}_P , \mathcal{G}_S and \mathcal{G}_P in section 3.2 and section 4. The perturbative differential cross section in P-wave channel at LO is given by

$$\begin{aligned}
& \frac{d\sigma_P^{LO}}{dz}(z, M_\psi, s, m_c) \\
&= \frac{128\pi^2\alpha^2\alpha_s e_c^2}{27s^4 M_\psi^3(1-r)(1+r)\left(\frac{M_\psi}{2} - m_c\right)^2\left(\frac{M_\psi}{2} + m_c\right)^4} \delta(1-\bar{z}) \left[\frac{M_\psi^{10}}{8} + \frac{3}{4}m_c M_\psi^9 \right. \\
&+ M_\psi^8 \left(\frac{1}{16}(18\mathcal{T}^2 - 60\mathcal{T} + 65)m_c^2 + \frac{5s}{32} \right) + M_\psi^7 \left(\frac{3}{16}s(7-2\mathcal{T})m_c + \frac{3}{2}(3\mathcal{T}^2 - 11\mathcal{T} + 7)m_c^3 \right) \\
&+ M_\psi^6 \left(-\frac{1}{4}s(9\mathcal{T}^2 - 12\mathcal{T} + 2)m_c^2 + \left(9\mathcal{T}^2 - 33\mathcal{T} + \frac{79}{8}\right)m_c^4 + \frac{3s^2}{16} \right) \\
&+ M_\psi^5 \left(\frac{3}{16}s^2(2\mathcal{T} + 1)m_c - \frac{3}{2}s(3\mathcal{T}^2 - 3\mathcal{T} + 5)m_c^3 + 6\mathcal{T}(3\mathcal{T} - 7)m_c^5 \right) \\
&+ M_\psi^4 \left(\frac{3}{16}s^2(6\mathcal{T}^2 - 20\mathcal{T} + 9)m_c^2 + \frac{1}{2}s(9\mathcal{T}^2 - 36\mathcal{T} + 8)m_c^4 + 3\mathcal{T}(15\mathcal{T} - 11)m_c^6 \right) \\
&+ M_\psi^3 \left(\frac{3}{2}s^2(1-4\mathcal{T})m_c^3 + 3s\mathcal{T}(3\mathcal{T} + 2)m_c^5 + 72\mathcal{T}^2 m_c^7 \right) \\
&+ M_\psi^2 \left(\frac{3}{2}s^2(3\mathcal{T}^2 - 5\mathcal{T} + 1)m_c^4 + 12s\mathcal{T}(3\mathcal{T} - 1)m_c^6 + 54\mathcal{T}^2 m_c^8 \right) + 9s^2\mathcal{T}^2 m_c^5 M_\psi \\
&+ 9s^2\mathcal{T}^2 m_c^6 \left. \right]. \tag{A.1}
\end{aligned}$$

The expressions of R_S , R_P , \mathcal{R}_S and \mathcal{R}_P are given as

$$\begin{aligned}
& R_S(M_\psi, r, \mu_r) \\
&= \frac{1}{4(1-r)(2-r)^2 N_c} \left[\frac{4}{3} (r-1) (r^2 N_c (N_c + 2n_f) - 8r (N_c n_f - N_c^2 + 3) + 8N_c n_f - 8N_c^2 + 36) \right. \\
&\quad \times \ln r + \frac{4}{3} (1-r)(r-2)^2 N_c (2n_f - 23N_c) \ln(1+r) + 16 (2r^2 N_c^2 - r (7N_c^2 + 2) + 7N_c^2 + 3) \\
&\quad \times (1-r) \ln(1-r) - 8(1-r)(r-2)^2 N_c^2 (2 \ln r \ln(1+r) - 4 \ln r \ln(1-r) - 4 \ln(1-r) \ln(1+r) \\
&\quad + \ln^2(1+r) + 4 \ln^2(1-r)) + 4(r-2)^2 ((r-2)N_c^2 + 1) \left(2 \ln(2-r) \ln r - \ln^2(2-r) \right. \\
&\quad \left. - 2\text{Li}_2 \left(\frac{r}{2-r} \right) \right) + 8(r-2)^2 (r (2N_c^2 - 1) - 2) \ln(1 - \sqrt{1-r}) \ln(1 + \sqrt{1-r}) \\
&\quad + 2r(r-2)^2 \ln^2 r + 24\sqrt{1-r}(r-2)^2 \ln \frac{1 - \sqrt{1-r}}{1 + \sqrt{1-r}} + \frac{4}{9} \left(3N_c(r-1)(r-2)^2 \right. \\
&\quad \times (2n_f - 11N_c) \ln \frac{4\mu_r^2}{M_\psi^2} + (1-r) \left(r^2 [2N_c n_f (6 \ln 2 - 5) + N_c^2 (31 - 66 \ln 2) + 90] \right. \\
&\quad \left. - 2r [4N_c n_f (6 \ln 2 - 5) + N_c^2 (71 - 150 \ln 2) + 9(19 + 4 \ln 2)] + 4 [2N_c n_f (6 \ln 2 - 5) \right. \\
&\quad \left. \left. + N_c^2 (40 - 75 \ln 2) + 27(3 + \ln 2)] \right) - 3\pi^2 (r-2)^2 [(5r-4)N_c^2 - 1] \right] \Bigg], \tag{A.2}
\end{aligned}$$

$$\begin{aligned}
& R_P(M_\psi, r, \mu_r) \\
&= \frac{1}{6(7r^2 + 2r + 3) N_c} \left[\left(-r^6 N_c (31N_c + 14n_f) + r^5 (94N_c n_f + 35N_c^2 + 240) \right. \right. \\
&\quad \left. \left. + r^4 (-230N_c n_f + 353N_c^2 - 1248) + r^3 (250N_c n_f - 811N_c^2 + 2124) \right. \right. \\
&\quad \left. \left. - 2r^2 (70N_c n_f - 127N_c^2 + 528) + 4r (22N_c n_f + 74N_c^2 - 57) - 48N_c n_f + 48N_c^2 + 24 \right) \right. \\
&\quad \times \frac{2 \ln r}{(r-2)^3 (r-1)} + 2(7r^2 + 2r + 3) N_c (2n_f - 23N_c) \ln(1+r) - 12N_c^2 (7r^2 + 2r + 3) \\
&\quad \times \left(4 \ln^2(1-r) + \ln^2(1+r) - 4 \ln r \ln(1-r) - 4 \ln(1-r) \ln(1+r) + 2 \ln r \ln(1+r) \right) \\
&\quad - \frac{12(7r^3 (2N_c^2 + 1) + r^2 (4N_c^2 - 25) + r (6N_c^2 - 3) - 3)}{(1-r)^{3/2}} \ln \frac{1 - \sqrt{1-r}}{1 + \sqrt{1-r}} \\
&\quad + \frac{6(3r^4 N_c^2 + r^3 (2 - 8N_c^2) + r^2 (17N_c^2 - 11) - 6rN_c^2 + 6N_c^2 - 3)}{(r-1)^2} \left(2\text{Li}_2 \left(\frac{r}{2-r} \right) \right. \\
&\quad \left. + \ln^2(2-r) - 2 \ln r \ln(2-r) \right) - \frac{12}{(r-1)^2} \left(r^4 (22N_c^2 - 3) + r^3 (7 - 32N_c^2) \right. \\
&\quad \left. + r^2 (9 - 10N_c^2) + r (5 - 4N_c^2) + 6 \right) \ln(1 - \sqrt{1-r}) \ln(1 + \sqrt{1-r}) \\
&\quad + \frac{24}{(r-2)^3 (r-1)} \left(16r^6 N_c^2 - r^5 (93N_c^2 + 20) + r^4 (191N_c^2 + 104) - r^3 (172N_c^2 + 177) \right. \\
&\quad \left. + r^2 (113N_c^2 + 88) + r (19 - 109N_c^2) + 42N_c^2 - 2 \right) \ln(1-r) + 3(5 - 3r)r \ln^2 r \\
&\quad + \frac{2}{3(r-2)^3 (r-1)^2} \left(-3(r-1)^2 (r(7r+2) + 3)(r-2)^3 N_c (2n_f - 11N_c) \ln \frac{4\mu_r^2}{M_\psi^2} \right. \\
&\quad \left. + (r-1) \left(r^6 [N_c^2 (217 - 390 \ln 2) + 14N_c n_f (6 \ln 2 - 5) + 414] \right. \right. \\
&\quad \left. \left. - r^5 [N_c^2 (1601 - 3138 \ln 2) + 94N_c n_f (6 \ln 2 - 5) + 2718 + 720 \ln 2] \right) \right.
\end{aligned}$$

$$\begin{aligned}
& + r^4 [N_c^2(4501 - 8994 \ln 2) + 230N_c n_f(6 \ln 2 - 5) + 6498 + 3744 \ln 2] \\
& - r^3 [19N_c^2(329 - 582 \ln 2) + 250N_c n_f(6 \ln 2 - 5) + 6858 + 6372 \ln 2] \\
& + 2r^2 [N_c^2(2561 - 2796 \ln 2) + 70N_c n_f(6 \ln 2 - 5) + 36(51 + 44 \ln 2)] \\
& + 4r [N_c^2(537 \ln 2 - 791) - 22N_c n_f(6 \ln 2 - 5) - 576 + 171 \ln 2] \\
& + 24 [N_c^2(49 - 75 \ln 2) + 2N_c n_f(6 \ln 2 - 5) + 54 - 3 \ln 2] \Big) + 3\pi^2(r - 2)^3 \\
& \times [N_c^2(39r^4 - 64r^3 + 19r^2 - 18r + 12) - 2r^3 + 11r^2 + 3] \Big), \tag{A.3}
\end{aligned}$$

$$\begin{aligned}
& \mathcal{R}_S(\bar{z}, M_\psi, r, \mu_r) \\
& = \frac{-2(1+r)}{(r\bar{z} + \bar{z} - 2)^2} \left[\frac{4n_f}{3} + \frac{N_c}{3(r\bar{z} - 2r + \bar{z})^2} \left((r+1)^2(6r-7)\bar{z}^2 - 4(9r^3 - 4r^2 - 10r + 3)\bar{z} \right. \right. \\
& \quad \left. \left. + 4(9r^3 - 10r^2 - 3r + 3) \right) + \ln \frac{\left(-\sqrt{(r+1)^2\bar{z}^2 - 4r} - r\bar{z} + 2r - \bar{z} \right)^2}{4r(r+1)(1-\bar{z})} \right. \\
& \quad \times \frac{2N_c}{(r\bar{z} - 2r + \bar{z})^3 \sqrt{(r+1)^2\bar{z}^2 - 4r}} \left((r+1)^5\bar{z}^5 - 2(r+1)^4(3r+2)\bar{z}^4 + 2(r+1)^3 \right. \\
& \quad \times (8r^2 + 9r + 3)\bar{z}^3 - 2(r+1)^2(12r^3 + 15r^2 + 12r + 1)\bar{z}^2 + 8r^2(3r^3 + 4r^2 + 7r + 6)\bar{z} \\
& \quad \left. \left. - 4r(3r^4 - 2r^3 + 6r^2 + 2r - 1) \right) \right], \tag{A.4}
\end{aligned}$$

$$\begin{aligned}
& \mathcal{R}_P(\bar{z}, M_\psi, r, \mu_r) \\
& = \frac{4(1+r)}{(r\bar{z} + \bar{z} - 2)^4(7r^2 + 2r + 3)} \left[\frac{2n_f}{3} \left((r+1)^2(3r^3 - 13r^2 - 4r - 4)\bar{z}^2 \right. \right. \\
& \quad \left. \left. + 4(-4r^4 + 7r^3 + 10r^2 + 2r + 3)\bar{z} + 2(3r^4 + 6r^3 - 25r^2 + 10r - 6) + r(r+1)^3(r+2)\bar{z}^3 \right) \right. \\
& \quad - \frac{N_c}{3(r\bar{z} - 2r + \bar{z})^4} \left(23r(r+1)^7(r+2)\bar{z}^7 - (r+1)^6(124r^3 + 577r^2 + 245r + 20)\bar{z}^6 \right. \\
& \quad - 2(r+1)^5(78r^4 - 1564r^3 - 1009r^2 - 364r - 39)\bar{z}^5 + 2(r+1)^4(880r^5 - 3032r^4 - 5533r^3 \\
& \quad - 1110r^2 - 823r - 42)\bar{z}^4 - 16r(r+1)^3(220r^5 - 92r^4 - 1663r^3 - 645r^2 - 88r - 147)\bar{z}^3 \\
& \quad + 8r(r+1)^2(333r^6 + 1108r^5 - 3476r^4 - 3248r^3 - 21r^2 - 270r - 222)\bar{z}^2 \\
& \quad - 16r(39r^8 + 596r^7 + 91r^6 - 2332r^5 - 1909r^4 - 94r^3 - 81r^2 - 102r - 72)\bar{z} + 32r(63r^7 \\
& \quad \left. \left. + 84r^6 - 362r^5 - 34r^4 - 39r^3 + 39r^2 - 18r - 9) \right) - \frac{N_c(1-r)}{(r\bar{z} - 2r + \bar{z})^5 \sqrt{(r+1)^2\bar{z}^2 - 4r}} \right. \\
& \quad \times \ln \frac{\left(-\sqrt{(r+1)^2\bar{z}^2 - 4r} - r\bar{z} + 2r - \bar{z} \right)^2}{4r(r+1)(1-\bar{z})} \left(3(r-1)(r+1)^9\bar{z}^9 - 2(r+1)^8(14r^2 - 9r - 11)\bar{z}^8 \right. \\
& \quad + 2(r+1)^7(93r^3 - 60r^2 - 94r - 35)\bar{z}^7 - 2(r+1)^6(406r^4 - 88r^3 - 641r^2 - 294r - 55)\bar{z}^6 \\
& \quad + 8(r+1)^5(288r^5 + 123r^4 - 523r^3 - 445r^2 - 105r - 10)\bar{z}^5 \\
& \quad + 16r^2(r+1)^3(262r^5 + 817r^4 - 475r^3 - 1091r^2 - 617r - 240)\bar{z}^3 \\
& \quad - 4(r+1)^4(1018r^6 + 1438r^5 - 1997r^4 - 2485r^3 - 1201r^2 - 129r - 4)\bar{z}^4 \\
& \quad - 16r(r+1)^2(137r^7 + 932r^6 + 12r^5 - 1282r^4 - 637r^3 - 400r^2 - 108r + 2)\bar{z}^2 \\
& \quad + 32r^2(13r^8 + 258r^7 + 457r^6 - 234r^5 - 647r^4 - 318r^3 - 181r^2 - 90r - 26)\bar{z} \\
& \quad \left. \left. - 64r^2(21r^7 + 56r^6 - 55r^5 - 42r^4 - 12r^3 - 3r^2 - 10r - 3) \right) \right]. \tag{A.5}
\end{aligned}$$

The functions \mathcal{G}_S and \mathcal{G}_P in eq.(4.7) are expressed as

$$\begin{aligned}
& \mathcal{G}_S(2m_c, r', \mu_r) \\
= & \frac{1}{36N_c} \left[\frac{24 \ln(1-r') (r'^2 N_c (2n_f - 11N_c) - 2r' (4N_c n_f - 25N_c^2 + 6) + 8N_c n_f - 50N_c^2 + 18)}{(r' - 2)^2} \right. \\
& - \frac{24}{(r' - 2)^2 (r' - 1)} \left(r'^3 N_c (2n_f - 11N_c) + r'^2 (-7N_c n_f + 55N_c^2 - 12) + r' (4N_c n_f - 76N_c^2 + 30) \right. \\
& \left. + 4N_c n_f + 26N_c^2 - 18 \right) \ln r' - \frac{24 (2N_c n_f - 5N_c^2 - 9) + 108r' (N_c^2 + 2)}{(1 - r')^{3/2}} \ln \frac{1 - \sqrt{1 - r'}}{1 + \sqrt{1 - r'}} \\
& + 144N_c^2 \text{Li}_2(r') + \frac{72 ((r' - 2)N_c^2 + 1)}{r' - 1} \text{Li}_2 \left(\frac{r'}{2 - r'} \right) + \frac{36 \ln^2(2 - r') ((r' - 2)N_c^2 + 1)}{r' - 1} \\
& - \frac{72 \ln r' \ln(2 - r') ((r' - 2)N_c^2 + 1)}{r' - 1} + 144N_c^2 \ln(1 - r') \ln r' + \frac{9 \ln^2 r' (r' (3N_c^2 - 2) - 2N_c^2)}{r' - 1} \\
& - \frac{36 \ln(1 - \sqrt{1 - r'}) \ln(1 + \sqrt{1 - r'}) (r' (7N_c^2 - 2) - 2(N_c^2 + 2))}{r' - 1} + \frac{4}{(r' - 2)^2 (r' - 1)} \\
& \times \left(-3(2n_f - 11N_c) (r' - 2)^2 (r' - 1) N_c \ln \frac{\mu_r^2}{m_c^2} - 16N_c n_f r'^3 + 12N_c n_f r'^3 \ln 2 \right. \\
& + 104N_c n_f r'^2 - 60N_c n_f r'^2 \ln 2 - 224N_c n_f r' + 96N_c n_f r' \ln 2 + 160N_c n_f - 48N_c n_f \ln 2 \\
& + 199N_c^2 r'^3 - 66N_c^2 r'^3 \ln 2 - 1019N_c^2 r'^2 + 366N_c^2 r'^2 \ln 2 + 1670N_c^2 r' + 3\pi^2 (r' - 2)^2 (r' N_c^2 - 1) \\
& - 600N_c^2 r' \ln 2 - 856N_c^2 + 300N_c^2 \ln 2 + 90r'^3 - 432r'^2 - 72r'^2 \ln 2 + 666r' + 180r' \ln 2 \\
& \left. - 324 - 108 \ln 2 \right) \Big], \tag{A.6}
\end{aligned}$$

$$\begin{aligned}
& \mathcal{G}_P(2m_c, r', \mu_r) \\
= & \frac{1}{36(7r'^2 + 2r' + 3)N_c} \left[\frac{36}{(r' - 1)^2} (3N_c^2 r'^4 + (2 - 8N_c^2) r'^3 + (17N_c^2 - 11) r'^2 - 6N_c^2 r' + 6N_c^2 \right. \\
& - 3) \ln^2(2 - r') - \frac{72 (3N_c^2 r'^4 + (2 - 8N_c^2) r'^3 + (17N_c^2 - 11) r'^2 - 6N_c^2 r' + 6N_c^2 - 3)}{(r' - 1)^2} \ln r' \\
& \times \ln(2 - r') + 288 (3r'^2 - 2r' + 2) N_c^2 \ln(1 - r') \ln r' + 288 (3r'^2 - 2r' + 2) N_c^2 \text{Li}_2(r') \\
& + \frac{72 (3N_c^2 r'^4 + (2 - 8N_c^2) r'^3 + (17N_c^2 - 11) r'^2 - 6N_c^2 r' + 6N_c^2 - 3)}{(r' - 1)^2} \text{Li}_2 \left(\frac{r'}{2 - r'} \right) \\
& + \frac{9 (6 (7N_c^2 - 1) r'^4 + (22 - 114N_c^2) r'^3 + 2 (51N_c^2 - 13) r'^2 + (10 - 19N_c^2) r' + 4N_c^2)}{(r' - 1)^2} \ln^2 r' \\
& - 36 \left((78N_c^2 - 6) r'^4 + (14 - 210N_c^2) r'^3 + 2 (89N_c^2 + 9) r'^2 + (10 - 91N_c^2) r' + 12 (N_c^2 + 1) \right) \\
& \times \frac{\ln(1 - \sqrt{1 - r'}) \ln(1 + \sqrt{1 - r'})}{(r' - 1)^2} + \left(6 (-62N_c^2 + n_f N_c - 14) r'^3 + (680N_c^2 - 68n_f N_c + 300) \right. \\
& \times r'^2 + (-613N_c^2 + 100n_f N_c + 36) r' + 74N_c^2 - 32n_f N_c + 36 \Big) \frac{6}{(1 - r')^{3/2}} \ln \frac{1 - \sqrt{1 - r'}}{1 + \sqrt{1 - r'}} \\
& - \left(2(8n_f - 65N_c) N_c r'^7 + (1113N_c^2 - 98n_f N_c - 240) r'^6 + (-3599N_c^2 + 150n_f N_c + 1488) r'^5 \right. \\
& + 3 (1825N_c^2 + 74n_f N_c - 1124) r'^4 + (-3901N_c^2 - 942n_f N_c + 3180) r'^3 + 2(611N_c^2 + 546n_f N_c \\
& \left. - 414) r'^2 - 4 (122N_c^2 + 130n_f N_c + 63) r' + 8 (40N_c^2 + 10n_f N_c + 3) \right) \frac{12 \ln r}{(r' - 2)^3 (r' - 1)^2}
\end{aligned}$$

$$\begin{aligned}
& + \left((14n_f - 65N_c) N_c r'^6 + (523N_c^2 - 94n_f N_c - 120) r'^5 + (-1499N_c^2 + 230n_f N_c + 624) r'^4 \right. \\
& + (1843N_c^2 - 250n_f N_c - 1062) r'^3 + 4(-233N_c^2 + 35n_f N_c + 132) r'^2 + (358N_c^2 - 88n_f N_c \\
& + 114) r' + 12(-25N_c^2 + 4n_f N_c - 1) \left. \right) \frac{24 \ln(1-r')}{(r'-2)^3(r'-1)} + \left(-3(r'-1)^2(7r'^2 + 2r' + 3) \right. \\
& \times (2n_f - 11N_c) N_c (r'-2)^3 \ln \frac{\mu_r^2}{m_c^2} + 3\pi^2(13N_c^2 r'^4 - 2(4N_c^2 + 1) r'^3 + (11 - 29N_c^2) r'^2 + 14N_c^2 r' \\
& - 2N_c^2 + 3)(r'-2)^3 + (r'-1) \left[2((851 - 195 \ln 2)N_c^2 + 2n_f N_c(-37 + 21 \ln 2) + 207) r'^6 \right. \\
& - 2((6743 - 1569 \ln 2)N_c^2 + (-581 + 282 \ln 2)n_f N_c + 9(151 + 40 \ln 2)) r'^5 \\
& + ((42155 - 8994 \ln 2)N_c^2 + 4(-926 + 345 \ln 2)n_f N_c + 3744 \ln 2 + 6498) r'^4 \\
& - ((66301 - 11058 \ln 2)N_c^2 + 4(-1579 + 375 \ln 2)n_f N_c + 6372 \ln 2 + 6858) r'^3 \\
& + ((56126 - 5592 \ln 2)N_c^2 + 280(-23 + 3 \ln 2)n_f N_c + 72(51 + 44 \ln 2)) r'^2 \\
& + 4((-6457 + 537 \ln 2)N_c^2 + 4(247 - 33 \ln 2)n_f N_c + 9(-64 + 19 \ln 2)) r' \\
& \left. + 8((713 - 225 \ln 2)N_c^2 + 4(-35 + 9 \ln 2)n_f N_c - 9(-18 + \ln 2)) \right] \frac{4}{(r'-2)^3(r'-1)^2} \Big]. \quad (\text{A.7})
\end{aligned}$$

B x_{\min} dependence in SGF

In this appendix, we discuss the x_{\min} dependence of the cross section in SGF approach. To this end, we calculate the quantity $d\sigma_{J/\psi}/dx_{\min}$. In following discussion we take the S-wave contribution as an example, while the P-wave contribution can be analyzed similarly. From eq. (2.8) we can derive the integrated cross section as

$$\begin{aligned}
\sigma_{J/\psi} &= \int dz \int_{\max[(z+\sqrt{z^2-4r})/2, x_{\min}]^1} \frac{dx}{x} H_{[1S_0^{[8]}]}(\hat{z}, M_\psi/x, s, m_c, x_{\min}/x, \mu_f) \\
&\quad \times F_{[1S_0^{[8]}] \rightarrow \psi}(x, M_\psi, m_c, \mu_f) + \dots, \quad (\text{B.1})
\end{aligned}$$

where \dots denotes the P-wave contribution and we will ignore it. Thus we have

$$\begin{aligned}
\frac{d\sigma_{J/\psi}}{dx_{\min}} &= \int dz \theta \left(z \leq \frac{x_{\min}^2 + r}{x_{\min}} \right) \left[-\frac{1}{x_{\min}} H_{[1S_0^{[8]}]}(z/x_{\min}, M_\psi/x_{\min}, s, m_c, 1, \mu_f) \right. \\
&\quad \times F_{[1S_0^{[8]}] \rightarrow \psi}(x_{\min}, M_\psi, m_c, \mu_f) + \int_{x_{\min}}^1 \frac{dx}{x} \\
&\quad \times \left(\frac{d}{dx_{\min}} H_{[1S_0^{[8]}]}(\hat{z}, M_\psi/x, s, m_c, x_{\min}/x, \mu_f) \right) F_{[1S_0^{[8]}] \rightarrow \psi}(x, M_\psi, m_c, \mu_f) \Big]. \quad (\text{B.2})
\end{aligned}$$

According to the matching relation in eq. (2.16) and the perturbative cross section results in section 3.2, we have

$$H_{[1S_0^{[8]}]}^{LO}(z, M_\psi, s, m_c, x_{\min}, \mu_f) = \frac{256\pi^2 \alpha^2 \alpha_s e_c^2 m_c^2 \mathcal{T}^2}{3s^2 M_\psi^3} \frac{1-r}{1+r} \delta(1-\bar{z}), \quad (\text{B.3})$$

and

$$\frac{d}{dx_{\min}} H_{[1S_0^{[8]}]}(z, M_\psi, s, m_c, x_{\min}, \mu_f) = \frac{1}{x_{\min}} H_{[1S_0^{[8]}]}^{LO}(z/x_{\min}, M_\psi/x_{\min}, s, m_c, 1, \mu_f)$$

$$\times F_{[1S_0^{[8]}] \rightarrow c\bar{c}[1S_0^{[8]}]}^{NLO}(x_{\min}, M_\psi, m_c, \mu_f) + \mathcal{O}(\alpha_s^3). \quad (\text{B.4})$$

Then up to order α_s^2 we find

$$\begin{aligned} \frac{d\sigma_{J/\psi}}{dx_{\min}} &= \int dz\theta \left(z \leq \frac{x_{\min}^2 + r}{x_{\min}} \right) \left[-\frac{1}{x_{\min}} \left(H_{[1S_0^{[8]}]}^{LO}(z/x_{\min}, M_\psi/x_{\min}, s, m_c, 1, \mu_f) \right. \right. \\ &\quad \left. \left. + H_{[1S_0^{[8]}]}^{NLO}(z/x_{\min}, M_\psi/x_{\min}, s, m_c, 1, \mu_f) \right) F_{[1S_0^{[8]}] \rightarrow \psi}(x_{\min}, M_\psi, m_c, \mu_f) \right. \\ &\quad \left. + \int_{x_{\min}}^1 \frac{dx}{x} \frac{x}{x_{\min}} H_{[1S_0^{[8]}]}^{LO}(z/(xx_{\min}), M_\psi/(xx_{\min}), s, m_c, 1/x, \mu_f) \right. \\ &\quad \left. \times F_{[1S_0^{[8]}] \rightarrow c\bar{c}[1S_0^{[8]}]}^{NLO}(x_{\min}/x, M_\psi/x, m_c, \mu_f) F_{[1S_0^{[8]}] \rightarrow \psi}(x, M_\psi, m_c, \mu_f) \right]. \quad (\text{B.5}) \end{aligned}$$

Let us first ignore the evolution of $F_{[1S_0^{[8]}] \rightarrow \psi}$, then it is natural to model $F_{[1S_0^{[8]}] \rightarrow \psi}$ as

$$\begin{aligned} F_{[1S_0^{[8]}] \rightarrow \psi}(x, M_\psi, m_c, \mu_f) &= \int_x^1 \frac{dy}{y} F_{[1S_0^{[8]}] \rightarrow c\bar{c}[1S_0^{[8]}]}(x/y, M_\psi/y, m_c, \mu_f) F^{\text{mod}}[1S_0^{[8]}](y) \\ &= F^{\text{mod}}[1S_0^{[8]}](x) + \int_x^1 \frac{dy}{y} F_{[1S_0^{[8]}] \rightarrow c\bar{c}[1S_0^{[8]}]}^{NLO}(x/y, M_\psi/y, m_c, \mu_f) F^{\text{mod}}[1S_0^{[8]}](y), \quad (\text{B.6}) \end{aligned}$$

where $F^{\text{mod}}[1S_0^{[8]}](y)$ is the inverse Laplace transform of the model $\tilde{F}^{\text{mod}}[1S_0^{[8]}](\nu)$ in eq. (3.10),

$$F^{\text{mod}}[1S_0^{[8]}](y) = \frac{1}{2\pi i} \int_{c-i\infty}^{c+i\infty} d\nu e^{(1/y-1)\nu} \tilde{F}^{\text{mod}}[1S_0^{[8]}](\nu). \quad (\text{B.7})$$

We assume $F^{\text{mod}}[1S_0^{[8]}](y)$ to be peaked around $y = 1$ and vanished at small and moderate y , i.e. $F^{\text{mod}}[1S_0^{[8]}](x_{\min}) \sim 0$. Besides, we assume the model function satisfies the moment relations [5, 26, 62]

$$\begin{aligned} \int_0^1 \frac{dy}{y^2} F^{\text{mod}}[1S_0^{[8]}](y) &= \mathcal{O}(1), \\ \int_0^1 \frac{dy}{y^2} \left(\frac{1}{y} - 1 \right) F^{\text{mod}}[1S_0^{[8]}](y) &= \mathcal{O}(\bar{\Lambda}/M_\psi), \\ \int_0^1 \frac{dy}{y^2} \left(\frac{1}{y} - 1 \right)^2 F^{\text{mod}}[1S_0^{[8]}](y) &= \mathcal{O}(\bar{\Lambda}^2/M_\psi^2), \quad (\text{B.8}) \end{aligned}$$

with $\bar{\Lambda} \sim \Lambda_{\text{OCD}}$. Inserting eq. (B.6) into eq. (B.5) we then obtain

$$\begin{aligned} \frac{d\sigma_{J/\psi}}{dx_{\min}} &= \int dz\theta \left(z \leq \frac{x_{\min}^2 + r}{x_{\min}} \right) \left[-\frac{1}{x_{\min}} H_{[1S_0^{[8]}]}^{LO}(z/x_{\min}, M_\psi/x_{\min}, s, m_c, 1, \mu_f) \right. \\ &\quad \times \int_{x_{\min}}^1 \frac{dy}{y} F_{[1S_0^{[8]}] \rightarrow c\bar{c}[1S_0^{[8]}]}^{NLO}(x_{\min}/y, M_\psi/y, m_c, \mu_f) F^{\text{mod}}[1S_0^{[8]}](y) \\ &\quad \left. + \int_{x_{\min}}^1 \frac{dy}{y} \frac{y}{x_{\min}} H_{[1S_0^{[8]}]}^{LO}(z/(yx_{\min}), M_\psi/(yx_{\min}), s, m_c, 1/y, \mu_f) \right. \end{aligned}$$

$$\times F_{[1S_0^{[8]}] \rightarrow c\bar{c}[1S_0^{[8]}]}^{NLO}(x_{\min}/y, M_\psi/y, m_c, \mu_f) F^{\text{mod}}[1S_0^{[8]}](y) \Big] + \mathcal{O}(\alpha_s^3). \quad (\text{B.9})$$

Expanding the functions $H_{[1S_0^{[8]}]}^{LO}$ and $F_{[1S_0^{[8]}] \rightarrow c\bar{c}[1S_0^{[8]}]}^{NLO}$ in $(1/y - 1)$ and using eq. (B.8), it is easy to find

$$\frac{d\sigma_{J/\psi}}{dx_{\min}} = \mathcal{O}(\alpha_s^3) + \mathcal{O}(\alpha_s^2 \bar{\Lambda}/M_\psi), \quad (\text{B.10})$$

which can be ignored in perturbative calculation. Because the difference between the resummed SGD and the SGD modeled in eq. (B.6) is $\mathcal{O}(\alpha_s^3)$, the above equation is also valid for resummed SGD. Thus we argue that the x_{\min} dependence of $\sigma_{J/\psi}$ is α_s or $\Lambda_{\text{QCD}}/M_\psi$ suppressed.

References

- [1] G. T. Bodwin, E. Braaten, and G. P. Lepage, *Rigorous QCD analysis of inclusive annihilation and production of heavy quarkonium*, *Phys. Rev.* **D51** (1995) 1125–1171 [[hep-ph/9407339](#)] [[InSPIRE](#)]. [Erratum: *Phys. Rev.* D55,5853(1997)].
- [2] Y.-Q. Ma and K.-T. Chao, *New factorization theory for heavy quarkonium production and decay*, *Phys. Rev.* **D100** (2019) 094007 [[arXiv:1703.08402](#)] [[InSPIRE](#)].
- [3] A.-P. Chen and Y.-Q. Ma, *Theory for quarkonium: from NRQCD factorization to soft gluon factorization*, *Chin. Phys. C* **45** (2021) 013118 [[arXiv:2005.08786](#)] [[InSPIRE](#)].
- [4] R. Li, Y. Feng, and Y.-Q. Ma, *Exclusive quarkonium production or decay in soft gluon factorization*, *JHEP* **05** (2020) 009 [[arXiv:1911.05886](#)] [[InSPIRE](#)].
- [5] A.-P. Chen, X.-B. Jin, Y.-Q. Ma, and C. Meng, *Fragmentation function of $g \rightarrow Q\bar{Q}(^3S_1^{[8]})$ in soft gluon factorization and threshold resummation*, *JHEP* **06** (2021) 046 [[arXiv:2103.15121](#)] [[InSPIRE](#)].
- [6] **BaBar**, B. Aubert *et al.*, *Measurement of J/ψ production in continuum e^+e^- annihilations near $\sqrt{s} = 10.6$ GeV*, *Phys. Rev. Lett.* **87** (2001) 162002 [[hep-ex/0106044](#)] [[InSPIRE](#)].
- [7] **Belle**, K. Abe *et al.*, *Production of prompt charmonia in e^+e^- annihilation at $s^{**}(1/2)$ is approximately 10.6-GeV*, *Phys. Rev. Lett.* **88** (2002) 052001 [[hep-ex/0110012](#)] [[InSPIRE](#)].
- [8] **Belle**, K. Abe *et al.*, *Observation of double c anti- c production in e^+e^- annihilation at $s^{**}(1/2)$ approximately 10.6-GeV*, *Phys. Rev. Lett.* **89** (2002) 142001 [[hep-ex/0205104](#)] [[InSPIRE](#)].
- [9] **Belle**, P. Pakhlov *et al.*, *Measurement of the $e^+e^- \rightarrow J/\psi c$ anti- c cross section at $s^{**}(1/2) \sim 10.6$ -GeV*, *Phys. Rev. D* **79** (2009) 071101 [[arXiv:0901.2775](#)] [[InSPIRE](#)].
- [10] V. Kiselev, A. Likhoded, and M. Shevlyagin, *Double charmed baryon production at B factory*, *Phys.Lett.* **B332** (1994) 411–414 [[hep-ph/9408407](#)] [[InSPIRE](#)].
- [11] E. Braaten and Y.-Q. Chen, *Signature for color octet production of J/ψ in e^+e^- annihilation*, *Phys.Rev.Lett.* **76** (1996) 730–733 [[hep-ph/9508373](#)] [[InSPIRE](#)].
- [12] F. Yuan, C.-F. Qiao, and K.-T. Chao, *Prompt J/ψ production at e^+e^- colliders*, *Phys.Rev.* **D56** (1997) 321–328 [[hep-ph/9703438](#)] [[InSPIRE](#)].

- [13] P. L. Cho and A. K. Leibovich, *Color singlet ψ_Q production at e^+e^- colliders*, *Phys.Rev.* **D54** (1996) 6690–6695 [[hep-ph/9606229](#)] [[InSPIRE](#)].
- [14] S. Baek, P. Ko, J. Lee, and H. Song, *Polarized J/ψ production at CLEO*, *J.Korean Phys.Soc.* **33** (1998) 97–101 [[hep-ph/9804455](#)] [[InSPIRE](#)].
- [15] G. A. Schuler, *Testing factorization of charmonium production*, *Eur. Phys. J. C* **8** (1999) 273–281 [[hep-ph/9804349](#)] [[InSPIRE](#)].
- [16] K.-Y. Liu, Z.-G. He, and K.-T. Chao, *Production of $J/\psi + c\bar{c}$ through two photons in e^+e^- annihilation*, *Phys.Rev.* **D68** (2003) 031501 [[hep-ph/0305084](#)] [[InSPIRE](#)].
- [17] K.-Y. Liu, Z.-G. He, and K.-T. Chao, *Inclusive charmonium production via double $c\bar{c}$ in e^+e^- annihilation*, *Phys.Rev.* **D69** (2004) 094027 [[hep-ph/0301218](#)] [[InSPIRE](#)].
- [18] Y.-J. Zhang and K.-T. Chao, *Double charm production $e^+e^- \rightarrow J/\psi + c\bar{c}$ at B factories with next-to-leading order QCD correction*, *Phys.Rev.Lett.* **98** (2007) 092003 [[hep-ph/0611086](#)] [[InSPIRE](#)].
- [19] B. Gong and J.-X. Wang, *Next-to-leading-order QCD corrections to $e^+e^- \rightarrow J/\psi + c\bar{c}$ at the B factories*, *Phys.Rev.* **D80** (2009) 054015 [[arXiv:0904.1103](#)] [[InSPIRE](#)].
- [20] Y.-Q. Ma, Y.-J. Zhang, and K.-T. Chao, *QCD correction to $e^+e^- \rightarrow J/\psi + g + g$ at B Factories*, *Phys.Rev.Lett.* **102** (2009) 162002 [[arXiv:0812.5106](#)] [[InSPIRE](#)].
- [21] B. Gong and J.-X. Wang, *Next-to-Leading-Order QCD Corrections to $e^+e^- \rightarrow J/\psi + g + g$ at the B Factories*, *Phys.Rev.Lett.* **102** (2009) 162003 [[arXiv:0901.0117](#)] [[InSPIRE](#)].
- [22] Z.-G. He, Y. Fan, and K.-T. Chao, *Relativistic correction to $e^+e^- \rightarrow J/\psi + gg$ at B factories and constraint on color-octet matrix elements*, *Phys. Rev. D* **81** (2010) 054036 [[arXiv:0910.3636](#)] [[InSPIRE](#)].
- [23] Y. Jia, *Color-singlet relativistic correction to inclusive J/ψ production associated with light hadrons at B factories*, *Phys. Rev. D* **82** (2010) 034017 [[arXiv:0912.5498](#)] [[InSPIRE](#)].
- [24] Y.-J. Zhang, Y.-Q. Ma, K. Wang, and K.-T. Chao, *QCD radiative correction to color-octet J/ψ inclusive production at B Factories*, *Phys.Rev.* **D81** (2010) 034015 [[arXiv:0911.2166](#)] [[InSPIRE](#)].
- [25] M. Beneke, I. Z. Rothstein, and M. B. Wise, *Kinematic enhancement of nonperturbative corrections to quarkonium production*, *Phys. Lett.* **B408** (1997) 373–380 [[hep-ph/9705286](#)] [[InSPIRE](#)].
- [26] S. Fleming, A. K. Leibovich, and T. Mehen, *Resumming the color octet contribution to $e^+e^- \rightarrow J/\psi + X$* , *Phys.Rev.* **D68** (2003) 094011 [[hep-ph/0306139](#)] [[InSPIRE](#)].
- [27] H.-S. Shao, *Initial state radiation effects in inclusive J/ψ production at B factories*, *JHEP* **04** (2014) 182 [[arXiv:1402.5840](#)] [[InSPIRE](#)].
- [28] Y.-Q. Ma, K. Wang, and K.-T. Chao, *$J/\psi(\psi')$ production at the Tevatron and LHC at $\mathcal{O}(\alpha_s^4 v^4)$ in nonrelativistic QCD*, *Phys.Rev.Lett.* **106** (2011) 042002 [[arXiv:1009.3655](#)] [[InSPIRE](#)].
- [29] M. Butenschoen and B. A. Kniehl, *Reconciling J/ψ production at HERA, RHIC, Tevatron, and LHC with NRQCD factorization at next-to-leading order*, *Phys.Rev.Lett.* **106** (2011) 022003 [[arXiv:1009.5662](#)] [[InSPIRE](#)].
- [30] B. Gong, L.-P. Wan, J.-X. Wang, and H.-F. Zhang, *Polarization for Prompt J/ψ , $\psi(2S)$*

- production at the Tevatron and LHC, *Phys.Rev.Lett.* **110** (2013) 042002 [[arXiv:1205.6682](#)] [[InSPIRE](#)].
- [31] G. T. Bodwin, H. S. Chung, U.-R. Kim, and J. Lee, *Fragmentation contributions to J/ψ production at the Tevatron and the LHC*, *Phys.Rev.Lett.* **113** (2014) 022001 [[arXiv:1403.3612](#)] [[InSPIRE](#)].
- [32] P. Faccioli, V. Knunz, C. Lourenco, J. Seixas, and H. K. Wohri, *Quarkonium production in the LHC era: a polarized perspective*, *Phys.Lett.* **B736** (2014) 98–109 [[arXiv:1403.3970](#)] [[InSPIRE](#)].
- [33] C. W. Bauer, S. Fleming, and M. E. Luke, *Summing Sudakov logarithms in $B \rightarrow X_s \gamma$ in effective field theory*, *Phys. Rev.* **D63** (2000) 014006 [[hep-ph/0005275](#)] [[InSPIRE](#)].
- [34] C. W. Bauer, S. Fleming, D. Pirjol, and I. W. Stewart, *An Effective field theory for collinear and soft gluons: Heavy to light decays*, *Phys. Rev.* **D63** (2001) 114020 [[hep-ph/0011336](#)] [[InSPIRE](#)].
- [35] C. W. Bauer and I. W. Stewart, *Invariant operators in collinear effective theory*, *Phys. Lett.* **B516** (2001) 134–142 [[hep-ph/0107001](#)] [[InSPIRE](#)].
- [36] C. W. Bauer, D. Pirjol, and I. W. Stewart, *Soft collinear factorization in effective field theory*, *Phys. Rev.* **D65** (2002) 054022 [[hep-ph/0109045](#)] [[InSPIRE](#)].
- [37] Y.-Q. Ma, J.-W. Qiu, and H. Zhang, *Fragmentation functions of polarized heavy quarkonium*, *JHEP* **06** (2015) 021 [[arXiv:1501.04556](#)] [[InSPIRE](#)].
- [38] M. Cacciari, P. Nason, and C. Oleari, *A Study of heavy flavored meson fragmentation functions in $e^+ e^-$ annihilation*, *JHEP* **04** (2006) 006 [[hep-ph/0510032](#)] [[InSPIRE](#)].
- [39] H. Shimizu, G. F. Sterman, W. Vogelsang, and H. Yokoya, *Dilepton production near partonic threshold in transversely polarized proton-antiproton collisions*, *Phys. Rev. D* **71** (2005) 114007 [[hep-ph/0503270](#)] [[InSPIRE](#)].
- [40] T. Hahn, *Generating Feynman diagrams and amplitudes with FeynArts 3*, *Comput.Phys.Commun.* **140** (2001) 418–431 [[hep-ph/0012260](#)] [[InSPIRE](#)].
- [41] C. Anastasiou and K. Melnikov, *Higgs boson production at hadron colliders in NNLO QCD*, *Nucl. Phys. B* **646** (2002) 220–256 [[hep-ph/0207004](#)] [[InSPIRE](#)].
- [42] C. Anastasiou, L. J. Dixon, and K. Melnikov, *NLO Higgs boson rapidity distributions at hadron colliders*, *Nucl. Phys. B Proc. Suppl.* **116** (2003) 193–197 [[hep-ph/0211141](#)] [[InSPIRE](#)].
- [43] C. Anastasiou, L. J. Dixon, K. Melnikov, and F. Petriello, *Dilepton rapidity distribution in the Drell-Yan process at NNLO in QCD*, *Phys. Rev. Lett.* **91** (2003) 182002 [[hep-ph/0306192](#)] [[InSPIRE](#)].
- [44] K. G. Chetyrkin and F. V. Tkachov, *Integration by Parts: The Algorithm to Calculate beta Functions in 4 Loops*, *Nucl. Phys.* **B192** (1981) 159–204 [[InSPIRE](#)].
- [45] S. Laporta, *High precision calculation of multiloop Feynman integrals by difference equations*, *Int. J. Mod. Phys. A* **15** (2000) 5087–5159 [[hep-ph/0102033](#)] [[InSPIRE](#)].
- [46] A. V. Smirnov, *FIRE5: a C++ implementation of Feynman Integral REduction*, *Comput. Phys. Commun.* **189** (2015) 182–191 [[arXiv:1408.2372](#)] [[InSPIRE](#)].
- [47] A. V. Kotikov, *Differential equations method: New technique for massive Feynman diagrams calculation*, *Phys. Lett.* **B254** (1991) 158–164 [[InSPIRE](#)].

- [48] T. Gehrmann and E. Remiddi, *Differential equations for two loop four point functions*, *Nucl. Phys.* **B580** (2000) 485–518 [[hep-ph/9912329](#)] [[InSPIRE](#)].
- [49] M. Beneke and V. A. Smirnov, *Asymptotic expansion of Feynman integrals near threshold*, *Nucl.Phys.* **B522** (1998) 321–344 [[hep-ph/9711391](#)] [[InSPIRE](#)].
- [50] R. N. Lee, *Reducing differential equations for multiloop master integrals*, *JHEP* **04** (2015) 108 [[arXiv:1411.0911](#)] [[InSPIRE](#)].
- [51] J. M. Henn, *Multiloop integrals in dimensional regularization made simple*, *Phys. Rev. Lett.* **110** (2013) 251601 [[arXiv:1304.1806](#)] [[InSPIRE](#)].
- [52] A. B. Goncharov, *Multiple polylogarithms and mixed Tate motives*, [[math/0103059](#)] [[InSPIRE](#)].
- [53] C. Duhr and F. Dulat, *PolyLogTools — polylogs for the masses*, *JHEP* **08** (2019) 135 [[arXiv:1904.07279](#)] [[InSPIRE](#)].
- [54] Q.-F. Sun, Y. Jia, X. Liu, and R. Zhu, *Inclusive h_c production and energy spectrum from e^+e^- annihilation at a super B factory*, *Phys. Rev.* **D98** (2018) 014039 [[arXiv:1801.10137](#)] [[InSPIRE](#)].
- [55] C. W. Bauer, C.-W. Chiang, S. Fleming, A. K. Leibovich, and I. Low, *Resumming the Color Octet Contribution to Radiative Upsilon Decay*, *Phys. Rev.* **D64** (2001) 114014 [[hep-ph/0106316](#)] [[InSPIRE](#)].
- [56] T. Becher and M. D. Schwartz, *Direct photon production with effective field theory*, *JHEP* **02** (2010) 040 [[arXiv:0911.0681](#)] [[InSPIRE](#)].
- [57] G. P. Korchemsky and A. V. Radyushkin, *Renormalization of the Wilson Loops Beyond the Leading Order*, *Nucl. Phys. B* **283** (1987) 342–364 [[InSPIRE](#)].
- [58] Z.-B. Kang, J.-W. Qiu, and G. Sterman, *Heavy quarkonium production and polarization*, *Phys.Rev.Lett.* **108** (2012) 102002 [[arXiv:1109.1520](#)] [[InSPIRE](#)].
- [59] Z.-B. Kang, Y.-Q. Ma, J.-W. Qiu, and G. Sterman, *Heavy quarkonium production at collider energies: Factorization and Evolution*, *Phys.Rev.* **D90** (2014) 034006 [[arXiv:1401.0923](#)] [[InSPIRE](#)].
- [60] Z.-B. Kang, Y.-Q. Ma, J.-W. Qiu, and G. Sterman, *Heavy Quarkonium Production at Collider Energies: Partonic Cross Section and Polarization*, *Phys.Rev.* **D91** (2015) 014030 [[arXiv:1411.2456](#)] [[InSPIRE](#)].
- [61] K. Lee and G. Sterman, *Power expansion for heavy quarkonium production at next-to-leading order in e^+e^- annihilation*, *JHEP* **09** (2020) 046 [[arXiv:2006.07375](#)] [[InSPIRE](#)].
- [62] S. Fleming, A. K. Leibovich, and T. Mehen, *Resummation of Large Endpoint Corrections to Color-Octet J/ψ Photoproduction*, *Phys. Rev.* **D74** (2006) 114004 [[hep-ph/0607121](#)] [[InSPIRE](#)].